GROUND-WATER AVAILABILITY FROM THE HAWI AQUIFER IN THE KOHALA AREA, HAWAII

By Mark R. Underwood, William Meyer, and William R. Souza

U.S. GEOLOGICAL SURVEY
Water-Resources Investigations Report 95-4113

Prepared in cooperation with the
DEPARTMENT OF WATER SUPPLY
COUNTY OF HAWAII

Honolulu, Hawaii
1995

U.S. DEPARTMENT OF THE INTERIOR
BRUCE BABBITT, Secretary

U.S. GEOLOGICAL SURVEY
Gordon P. Eaton, Director

For sale by the U.S. Geological Survey
Earth Science Information Center
Open-File Reports Section
Box 25286, MS 517
Denver Federal Center
Denver, CO 80225

For additional information write to:
District Chief
U.S. Geological Survey
677 Ala Moana Blvd., Suite 415
Honolulu, HI 96813

CONTENTS

FIGURES

FIGURES--Continued

TABLES

Conversion Factors

Multiply	By	To obtain
acre	4,047	square meter
foot (ft)	0.3048	meter
foot per mile (ft/mi)	0.1894	meter per kilometer
foot per day (ft/d)	0.3048	meter per day
foot per day per foot (ft/d)/ft	1	meter per day per meter
cubic foot per second (ft^3/s)	0.02832	cubic meter per second
gallon per minute (gal/min)	0.06308	liter per second
million gallons per day (Mgal/d)	0.04381	cubic meter per second
mile (mi)	1.609	kilometer
square mile (mi^2)	2.590	square kilometer
inch (in.)	25.4	millimeter
inch per year (in/yr)	25.4	millimeter per year

Temperature is given in degrees Celsius (°*C*), which can be converted to degrees Fahrenheit (°*F*) by using the equation:

$$^{\circ}F = (1.8 \times {}^{\circ}C) + 32$$

Abbreviations used in water quality descriptions:

µg/L, micrograms per liter
mg/L, milligrams per liter
µS/cm, microsiemens per centimeter at 25° Celsius
ppm, parts per million
gm/cm^3, grams per cubic centimeter

GROUND-WATER AVAILABILITY FROM THE HAWI AQUIFER IN THE KOHALA AREA, HAWAII

by

Mark R. Underwood, William Meyer, and William R. Souza

ABSTRACT

A ground-water study consisting of test-well drilling, aquifer tests, and numerical simulation was done to investigate ground-water availability in the basal part of the Hawi aquifer between the western drainage divide of Pololu Valley and Upolu Point in Kohala, Hawaii. The test well drilling provided information on geology, water levels, water quality, vertical extent of the freshwater, and the thickness of the freshwater-saltwater transition zone in that aquifer. A total of 12 test wells were drilled at eight locations. Aquifer tests were done at five locations to estimate the hydraulic conductivity of the aquifer. Using information on the distribution of recharge, vertical extent of freshwater, hydraulic conductivity, and geometry of the basal aquifer, a numerical model was used to simulate the movement of water into, through, and out of the basal aquifer, and the effect of additional pumping on the water levels in the aquifer.

Results of the modeling indicate that ground-water withdrawal of 20 million gallons per day above the existing withdrawal of 0.6 million gallons per day from the basal aquifer is hydrologically feasible, but that spacing, depth, and pumping rates of individual wells are important. If pumping is concentrated, the likelihood of saltwater intrusion is increased. The additional withdrawal of 20 million gallons per day would result in a reduction of ground-water discharge to the ocean by an amount equal to pumpage. Although model-calculated declines in water-level outside the area of pumping are small, pumping could cause some reduction of streamflow near the mouth of Pololu Stream.

INTRODUCTION

The Kohala area of the island of Hawaii is the northwest peninsula of the island (fig. 1). The area is dominated by the asymmetrical, elongated Kohala Mountain. Kohala Mountain is an extinct volcanic dome reaching an altitude of 5,605 ft and is the oldest of the five volcanoes forming the island. The Hawaii Water Resources Protection Plan (George A.L. Yuen and Associates, Inc., 1992) delineated three aquifer systems in the Kohala area: Hawi, Waimanu, and Mahukona (fig. 1). Ground water in these systems is found as basal ground water along the flanks of the volcanic dome, and as high-level water in the rift zones (Stearns and Macdonald, 1946) (fig. 2). The basal ground water extends from the outer edges of the rift zones to a discharge area seaward of the shoreline, and is a roughly lens-shaped body of freshwater floating on seawater. The maximum altitude of the water table of the basal water is unknown.

The windward (northern) side of Kohala Mountain is relatively cool and wet, receiving more than 160 in/yr of rainfall near the summit (fig. 3). The leeward (southern) side of the mountain is in the rain shadow of Kohala Mountain. Average rainfall is less than 10 in/yr along the coast near Kawaihae. Tourism on the leeward side of the Kohala area is expected to grow considerably because of the dry, warm climate. One of the primary limitations for growth and development in this area is the availability of water. The Hawaii County Department of Water Supply (DWS) estimates that water demand in the year 2005 will increase by about 20 Mgal/d more than the present use of 0.6 Mgal/d (Thompson, 1988). Ground water is the preferred source to supply the projected demand, because of its quality, reliability, and lack of required treatment as compared with surface water.

To address an increased demand for water, the DWS and the U.S. Geological Survey (USGS) began a cooperative study to investigate ground-water availability from the basal part of the Hawi aquifer. This area was selected because of its high rainfall and because of the known existence of an extensive basal aquifer. This report describes the results of the study and includes a summary of exploratory well drilling and aquifer tests, and numerical simulation of the changes in the aquifer resulting from increased pumpage of 20 Mgal/d.

Scope

The primary study area for the field investigations was the basal part of the Hawi aquifer between the western drainage divide of Pololu Stream and Upolu Point (fig. 1). This basal aquifer extends to the southeast beyond the Pololu drainage divide and is contiguous with the basal part of the Waimanu aquifer. The Waimanu aquifer was not considered for ground-water development because of its rugged terrain; however, the Pololu drainage basin, which is within the Waimanu aquifer (fig. 1), was included in the numerical ground-water flow model constructed for this study. Because the basal aquifers are part of a larger ground-water system within the Kohala area, it was necessary to quantify rates of ground-water movement into the basal aquifers from areas adjacent

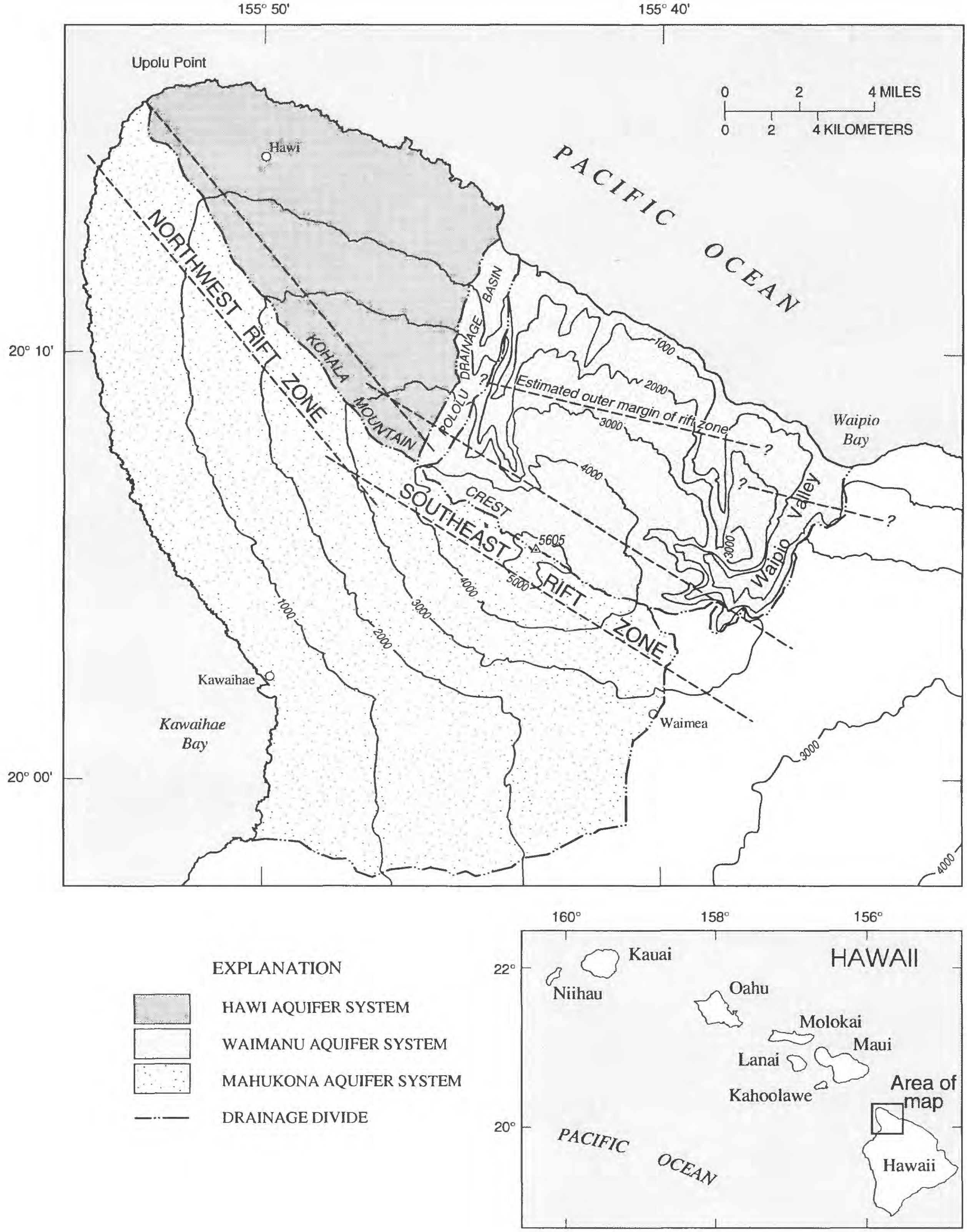

Figure 1. Hawaiian islands and aquifer systems in the Kohala area, island of Hawaii (aquifer systems are from George A. L. Yuen and Associates, Inc., 1992).

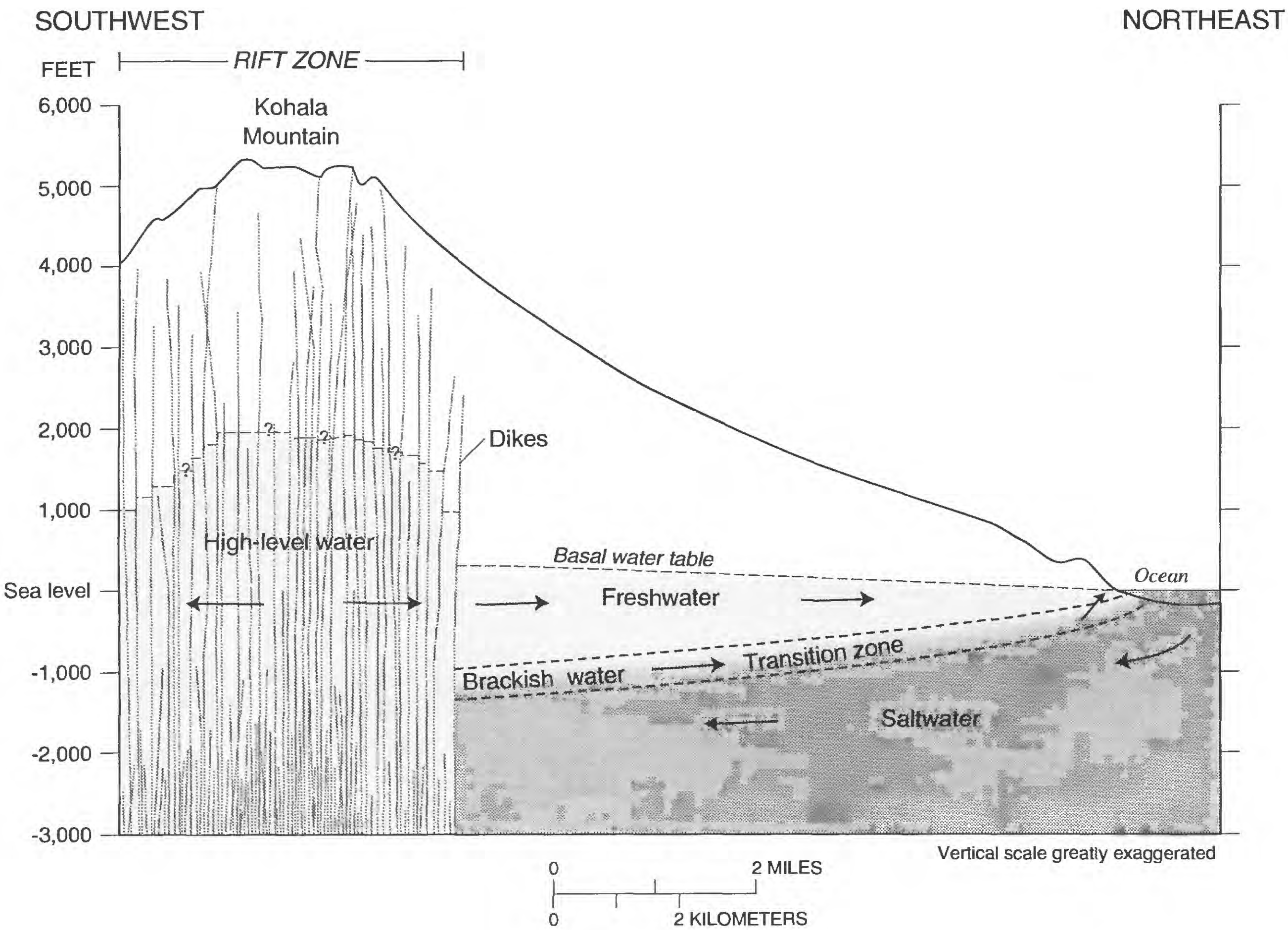

Figure 2. Generalized section of Kohala Mountain showing basal aquifer and direction of ground-water movement.

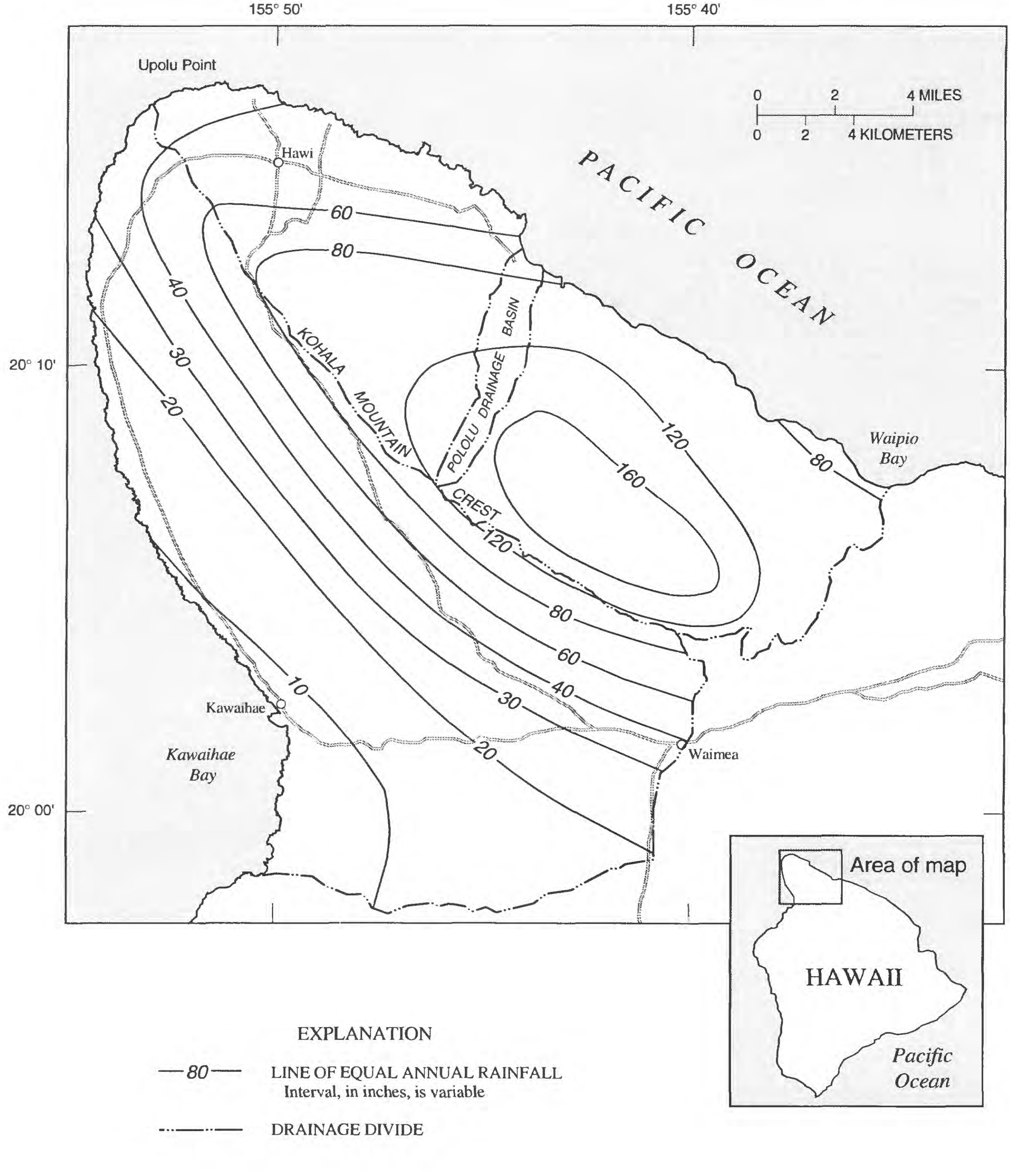

Figure 3. Mean annual rainfall, Kohala area, island of Hawaii (from Giambelluca and others, 1986).

to the basal aquifers. This information was provided in a study of ground-water recharge for the entire Kohala area by Shade (in press).

A program of test-well drilling was instituted in the Hawi basal aquifer to obtain information on geology, water levels, water quality, and vertical extent of freshwater and the transition zone. A total of 12 test wells were drilled at eight locations at altitudes ranging from about 108 to 630 ft above sea level (see fig. 7). Aquifer tests were done at five locations to estimate the horizontal hydraulic conductivity of the aquifer. Using information on the distribution of recharge, vertical extent of freshwater, horizontal hydraulic conductivity, and geometry of the basal aquifer, a numerical model was constructed to simulate the movement of water into, through, and out of the basal aquifer.The model was then used to estimate the hydrologic feasibility of developing 20 Mgal/d of fresh ground water in addition to the existing use of 0.6 Mgal/d.

Previous Investigations

Early studies in the Kohala area focused on streamflow in the area southeast of Pololu Stream. During a 10-month period in 1890, Lydgate measured streamflow in Waipio Valley (Davis and Yamanaga, 1963). During a 5-month period in 1889 and 1890, Brunner (Davis and Yamanaga, 1963) measured flow in the 17 streams that are tributary to Honokane Nui Stream (fig. 4). In 1901 and 1902, Tuttle (Martin and Pierce, 1913) investigated water resources in the Honokane Nui and Waipio Valleys as well as regions southeast of Waipio Valley by collecting information on streamflow, springs, and wells. Systematic streamflow measurement in the Kohala area was begun in 1907. Since 1912, stream and irrigation discharge ditch data have been published annually by the USGS. Many of the stream and ditch measurements were discontinued when sugarcane production was halted in the early 1970's.

The geology and ground-water resources of the island of Hawaii were described by Stearns and Macdonald (1946) who also provided a conceptual model of the hydrologic system of the Kohala area. Hydrologic information provided by Stearns and Macdonald (1946) was updated by Davis and Yamanaga (1963). A thorough inventory of basic water resources and historical records was compiled by the State of Hawaii (1970).

A project by the Kohala Sugar Company in 1964 drilled five successful observation holes into the Hawi basal aquifer between Upolu Point and Pololu Stream (Bowles and others, 1974). A water-level map was drawn from the data obtained from these holes and from existing data from wells in the area. Bowles and others (1974) evaluated surface-water and ground-water resources in the Kohala area with a focus on the flow in the Kohala ditch (fig. 4). Using a simplified water budget and Darcy's law they estimated that 40 to 45 Mgal/d flowed through the Hawi aquifer; of that quantity, 30 to 35 Mgal/d (75 percent of flow through the system) was available for development.

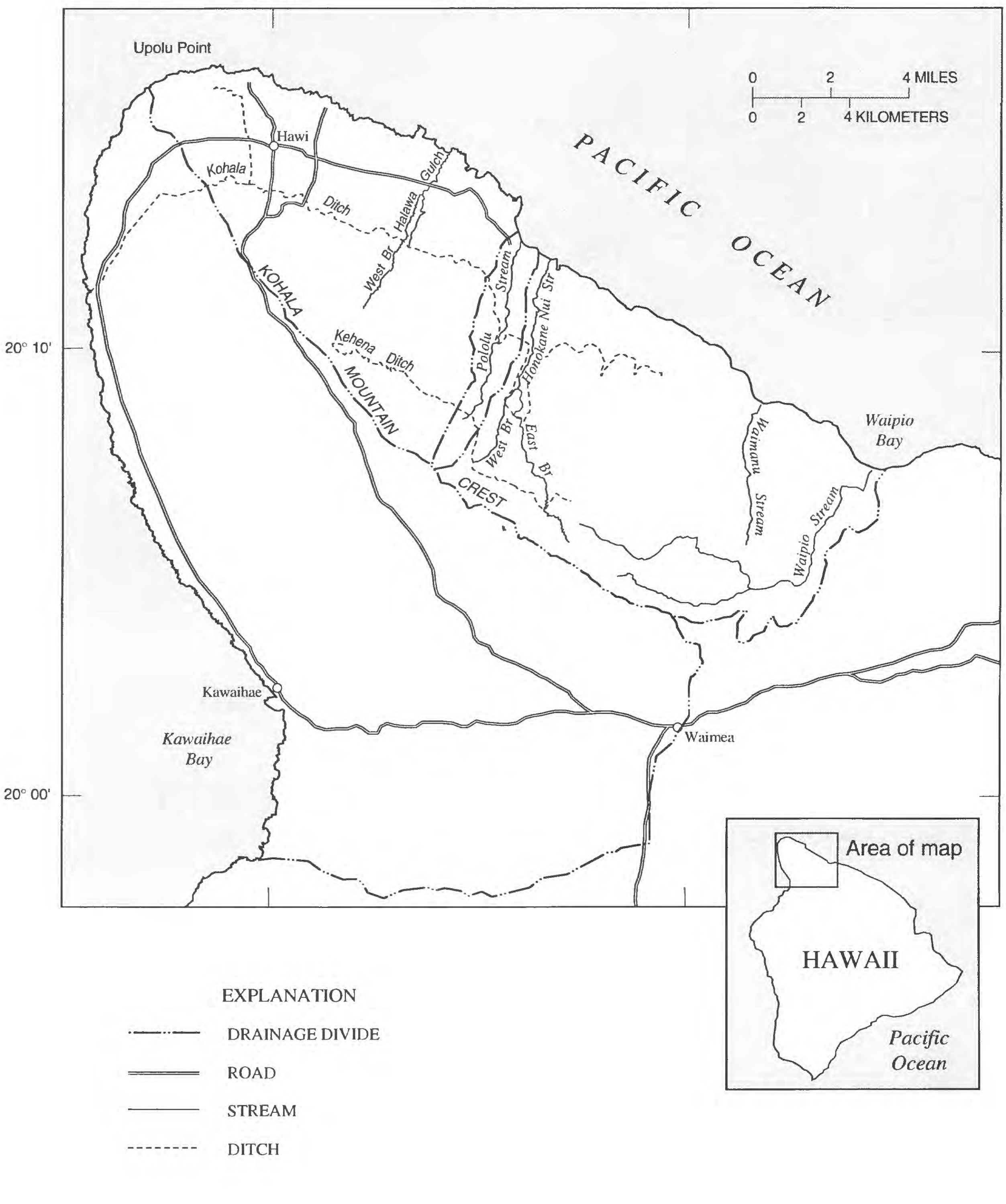

Figure 4. Streams, ditches, and tunnels in the Kohala area, island of Hawaii.

DESCRIPTION OF STUDY AREA

The Hawi basal aquifer is bounded along the southeast by the Pololu drainage divide and along the north and northwest by the Pacific Ocean. The southern and southwestern boundary is the rift zone along the crest of Kohala Mountain that extends from the summit toward the coast near Upolu Point (fig. 1). A slightly extended study area for modeling purposes included the continuation of the basal aquifer into the drainage area of Pololu Stream (fig. 4).

Altitude of the land surface on the Kohala Mountain increases gradually from sea level at the shoreline to 5,605 ft above sea level at the mountain summit (fig. 1). In general, the surface relief of the study area is moderately dissected. It is covered dominantly by pastures and orchards, with forests covering upland areas. Sugarcane was produced over much of this area from the early 1900's until the early 1970's. Two major irrigation ditches, Kohala and Kehena (fig. 4), were constructed in the early 1900's to transport water from the area east of Pololu Stream into the study area to support agriculture.

The Kohala ditch, constructed in 1901–02 by the Kohala Sugar Company, presently diverts water from the east branch of Honokane Nui Stream at an altitude of 2,000 ft. The ditch carries the water for 18 mi northwest, mostly as tunnel, toward Hawi where it delivers most of its water to the intake of a hydroelectric plant near Hawi (fig. 4). The ditch also captures minor flows from springs and streams west of Pololu Stream.

During 1928–60, median monthly flow rates in the Kohala ditch out of Honokane Nui Stream ranged from 21.9 to 31.9 Mgal/d (Bowles and others, 1974). Present flow rates are about 10 to 15 Mgal/d. Much of the decline in flow in recent years can be attributed to the loss of water previously derived from streams east of Honokane Nui Stream. At the hydroelectric plant at Hawi, the water released by the plant is injected into the basal aquifer through a holding pond into a row of five shallow injection wells located about 1.7 mi inland at about 520 ft altitude. Depths of these injection wells range from 160 to 240 ft altitude and lateral spacing between them is about 35 ft. The average rate of injection is about 8 Mgal/d.

The Kehena ditch diverts water from an intake at Honokane Nui Stream above the canyon rim at an altitude of about 4,200 ft (fig. 3) and carries the water westward for about 8 mi. Discharge measurements were made in the ditch from 1917 through 1919 and from 1928 through 1966. Average discharge in the ditch for these periods was 7.38 Mgal/d. In recent years the ditch has fallen into disrepair and does not flow continuously.

The extended study area, included for purposes of ground-water modeling, contains the Pololu Stream drainage area. As discussed by Stearns and Macdonald (1946, p. 228), the source of water in Pololu Stream is from springs in its canyon walls below the dike zone and Stearns and Macdonald have described these springs as perched. Pololu Stream is sufficiently entrenched near the ocean to presumably intersect the basal aquifer. If this occurs, the area near the mouth of the stream would be expected to gain water from the Waimanu basal aquifer.

The geohydrologic setting of that part of the Waimanu aquifer beyond Pololu Valley is highly complex and to some extent poorly understood. The work of Stearns and Macdonald (1946) remains the definitive report for the area, but even so, the extent of the high-level and basal aquifers and the relation between surface water and ground water is unclear. Stearns mapped numerous dikes and dike-associated springs and described an area of high-level water about 6 mi wide underlying the higher part of Kohala Mountain (Stearns and Macdonald, 1946, p. 228). This width would extend the high-level aquifer considerably into the Waimanu aquifer. Stearns' description, however, does not allow the extent of the high-level aquifer to be closely delineated. Ground water discharging from behind dikes causes streams to gain along their entire course to the ocean, indicating that most of the area may consist of high-level water. However, Stearns and Macdonald mapped much of the area as basal aquifer. Three streams, Pololu, Waimanu, and Waipio may intersect the basal aquifer near the ocean, but the other streams are hundreds to thousands of feet above sea level along their entire courses and discharge to the ocean from high cliffs.

GEOLOGY

Kohala Mountain was formed by volcanic rocks derived from the now-extinct Kohala Volcano. The mountain is composed mainly of basaltic and andesitic (Pololu Basalt and Hawi Volcanics, respectively) lavas that erupted from two main rift zones that trend N 35° W and S 65° E from Kohala summit. These rift zones are referred to as the northwest and southeast rift zones, respectively. The estimated location and orientation of the central part of the rift zones are shown in figure 5. The estimated outer margin of the rift zone in the Waimanu aquifer, on the basis of mapped dikes (Stearns and Macdonald, 1946, plate 1), is also shown (figs. 1 and 5). The southern flanks of Kohala Mountain merge with Mauna Kea Volcano and form a saddle that slopes toward the eastern and western coasts of the island of Hawaii.

Pololu Basalt.--The Pololu Basalt contains a thick sequence of basalt lava flows composed of hundreds of individual pahoehoe and aa lava flows that range from a few to 50 ft in thickness and dip from 3 to 10 degrees away from the rift area (Stearns and Macdonald, 1946, p. 174). The basal aquifer is contained within lava flows of the Pololu Basalt. Lavas of the Pololu Basalt make up most of Kohala Mountain above sea level, and, because of subsidence of the island, extend an unknown distance below sea level.

Most of the eruptive areas of the Pololu Basalt have been buried by later lava flows of the Hawi Volcanics. Typically the upper 50 to 200 ft of the Pololu Basalt is decomposed from weathering processes (Stearns and Macdonald, 1946, p. 174). Greater weathering occurred in the wet areas and where the rocks were not covered by the later flows. Intercalated soils greater than a few inches thick are rare below the upper part of the Pololu Basalt, indicating that periods of time between flows were short. Thin vitric ash beds can be found throughout the basalts but rarely on the windward slopes of Kohala Mountain (Stearns and Macdonald, 1946).

In general, the Pololu Basalt resembles the Koolau Basalt on Oahu, which forms aquifers with high transmissivities. The clinker areas on either side of aa flows have high horizontal hydraulic conductivities as do the interflow faces between pahoehoe flows, fractures, and cooling joints in the rock. Because these lavas are layered and nearly horizontal, horizontal hydraulic conductivity is likely to be greater than the vertical hydraulic conductivity. Aquifer tests and numerical studies in the Pearl Harbor aquifer of Oahu indicate that the greatest-to-least (horizontal-to-vertical) hydraulic conductivity ratios, or anisotropy ratios, are from 10:1 to 1,000:1. In an analysis of the Pearl Harbor aquifer, Souza and Voss (1989) estimated a ratio of horizontal to vertical hydraulic conductivity of 200:1.

Intrusive dikes cut the Pololu Basalt flows in the deep canyons on the northeast slope. Dikes trend N 50° to 80° W and dip about 75° northeast (Stearns and Macdonald, 1946, p. 175). Widths of Pololu dikes range from a few inches to 10 ft and average about 2 ft. Dike concentrations become greater with depth and closeness to the rift areas. Their dense composition, late-stage intrusion, and

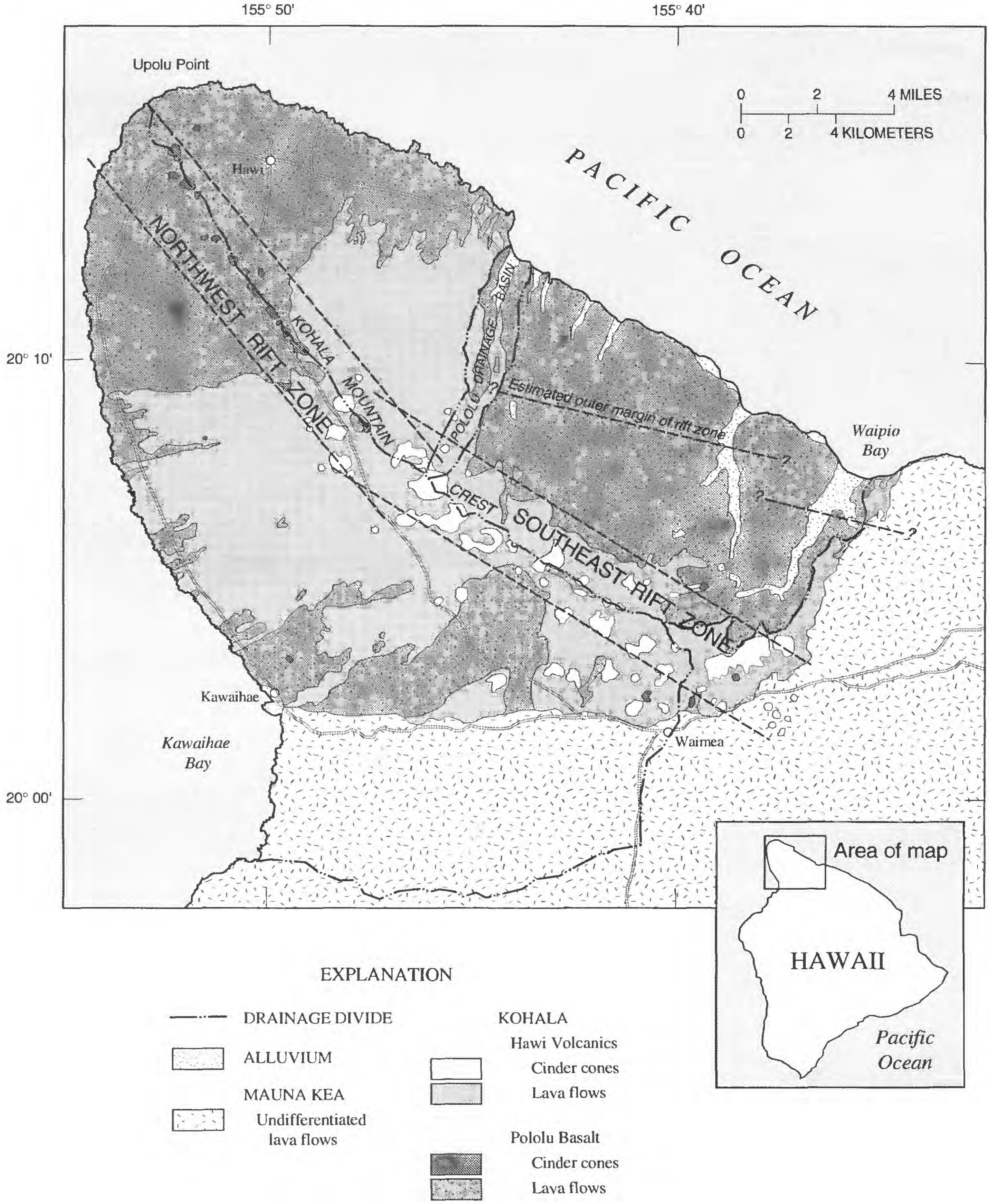

Figure 5. Surficial geology of the Kohala area, island of Hawaii (modified from Langenheim and Clague, 1987; and Stearns and Macdonald, 1946).

near-vertical emplacement give dikes relatively low horizontal hydraulic conductivity that impedes ground-water flow. On the basis of a description of the area between Pololu Stream and Waipio Stream (fig. 4) by Stearns and Macdonald (1946), the northern margin of the southeast rift zone, and the associated high-level water, may extend more than 4 mi from the summit area towards the ocean (fig. 5). As discussed, Stearns and Macdonald (1946) indicate a total width of about 6 mi for high-level water in the area of the Waimanu aquifer.

Hawi Volcanics.--The Hawi Volcanics form a cap over most of the rift zone and cover about a third of the northeast slope and about half of the southwest slope below the rift zone (fig. 5). Lava flows of the Hawi Volcanics were composed almost entirely of highly viscous aa that flowed onto the existing Pololu Basalt surface. An unconformity, that in places is marked by a red soil, exists between the Pololu Basalt and the overlying Hawi Volcanics. The red soil prevails on the southeastern slopes and indicates that most of the original topographic slopes were not eroded before being covered by lava flows of the Hawi Volcanics.

Only a few lava flows of the Hawi Volcanics extend to the coast. Thickness of individual lava flows range from 10 to 150 ft and average about 40 ft. In up-slope areas, flows overlap to reach a composite thickness as great as 500 ft near the summit. Many of the Hawi flows followed existing topography and filled the shallow canyons. Thin, ashy soils and gravel can be found between individual Hawi flows indicating longer periods of time between flows than in the Pololu Basalt. Soils that form on Hawi rocks are gray and can exceed 3 ft in thickness. These soils support agriculture when adequate moisture is present.

Alluvium.-- Alluvial deposits are found in the floors of the larger canyons on the windward side of Kohala Mountain (Stearns and Macdonald, 1946). These deposits consist of unconsolidated deposits of poorly sorted silts, sands, and boulders; landslide deposits characterized by blocks of volcanic rock in an earthy mix; and consolidated alluvium consisting of poorly sorted boulder conglomerates that form terraces in the lower stretches of the larger canyons and gulches. Stearns and Macdonald (1946, p. 172) indicate a thickness for the consolidated alluvium on the order of 500 ft and thickness of the unconsolidated deposits of about 25 ft. Both deposits are thought to be poorly permeable.

GROUND-WATER OCCURRENCE

The general movement of water in the Kohala area is from the mountainous areas toward the ocean. A schematic representation of this movement is shown in figure 2. In the mountainous areas, the movement of water is impeded by the presence of dikes within the rift zones. This impedance results in relatively high water levels in the rift zone that can be more than 2,000 ft above sea level (Stearns and Macdonald, 1946). Orientation of dikes is subparallel to the main orientation of the rift zone so that intersecting dikes are common and ground water is compartmentalized between the dikes. In Hawaii, this water is referred to as high-level water.

The water budget for the study area was estimated by Shade (in press). The major source of water to the basal part of the Hawi aquifer is from direct infiltration of precipitation. Recharge derived from this source is 53.1 Mgal/d on a mean annual basis. The movement of water into the basal aquifer from the adjacent rift zone constitutes another source of water that equals 6.9 Mgal/d on a mean annual basis. Mean annual recharge from infiltration of precipitation falling on the basal aquifer in the Pololu Stream drainage area is 7.2 Mgal/d and mean annual recharge to this aquifer from the rift zone above it is 1.2 Mgal/d. The actual rate of recharge at any point is dependent on the rate of precipitation minus water lost to evapotranspiration, direct runoff, and soil-moisture storage. Each of these factors varies from location to location. The areal distribution of ground-water recharge for the entire area is shown in figure 6.

A small amount of ground-water recharge is derived from water that infiltrates from the Kohala ditch. Discharge measurements made in the ditch during this study indicate a seepage loss ranging from 0.16 to 0.33 Mgal/d per mile with a total loss of about 2.0 Mgal/d in the study area. An additional source of recharge to the aquifer is derived from the injection of an estimated 8 Mgal/d at the Hawi hydroelectric plant.

Ground water moves out of the rift zone into the basal aquifer where the direction of ground-water motion is mainly horizontal. The altitudes of water levels in the basal aquifer measured on March 22, 1990 in the test wells drilled for this study ranged from a high of 11.3 ft above sea level to a low of 2.5 ft (fig. 7). Water levels higher than those shown in figure 7 would be expected inland toward the rift zone. As indicated by the water levels, there is a general northerly movement of water in the basal aquifer. Existing hydrologic conditions in the basal aquifer in terms of recharge to and discharge from the aquifer have not changed significantly for many years, indicating that water levels shown in figure 7 would represent equilibrium or near equilibrium conditions, although seasonal variations in water levels would be expected. Extensive agriculture and irrigation of crops ceased in the mid-1970's and water previously used for irrigation has been injected at the Hawi hydroelectric plant since about 1979. The only regularly pumped well in the basal aquifer is the DWS well. Production at this well (7449-02; see fig. 9) averages about 0.6 Mgal/d. Water levels were regularly measured in shaft 7652-01 from 1972 to 1995 and periodically measured in well 7347-02 (see fig. 9) from 1986 to February 1991 (fig. 8). This data supports the concept that equilibrium conditions exist in the aquifer.

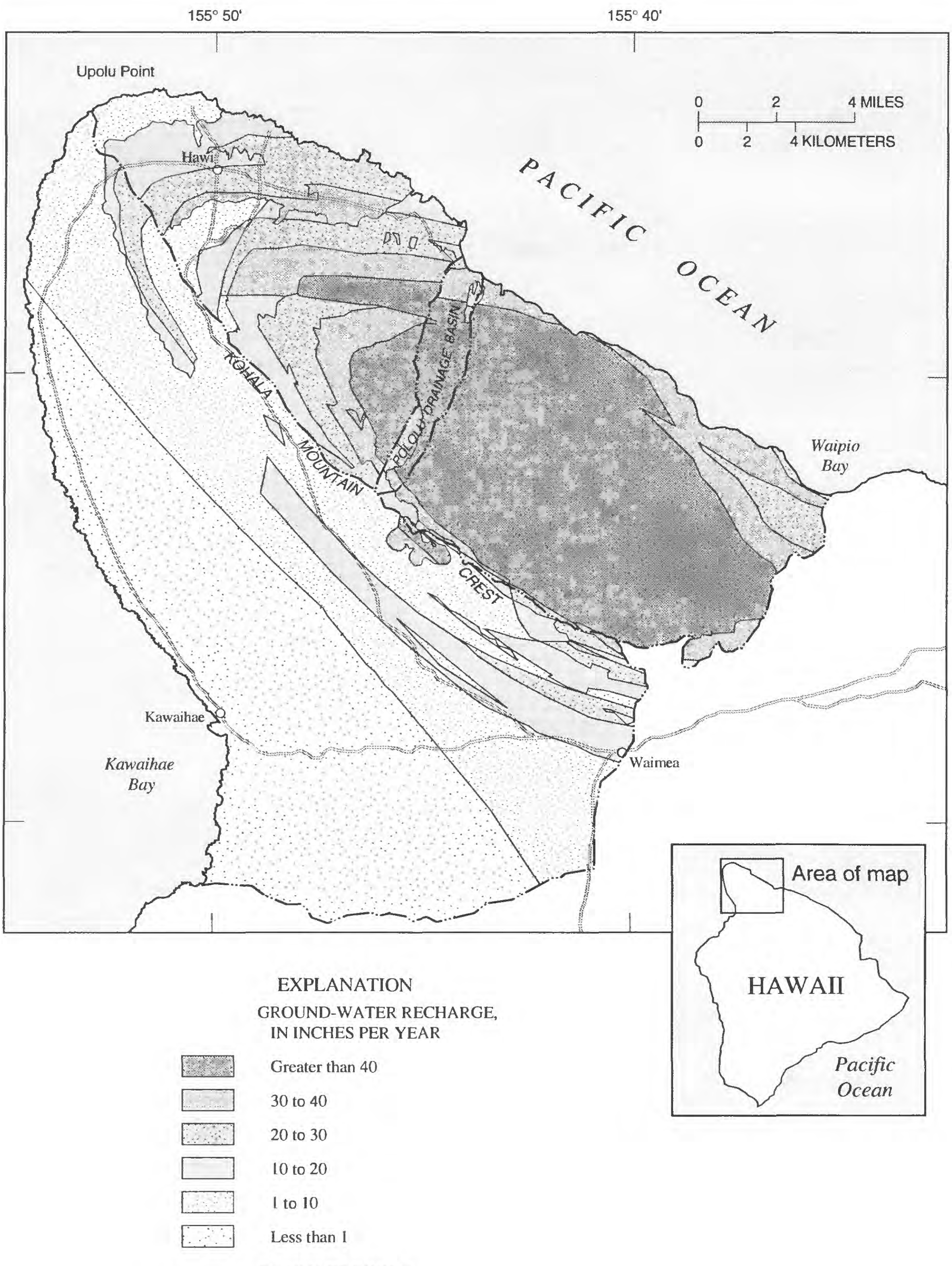

Figure 6. Ground-water recharge, Kohala area, island of Hawaii (Shade, in press).

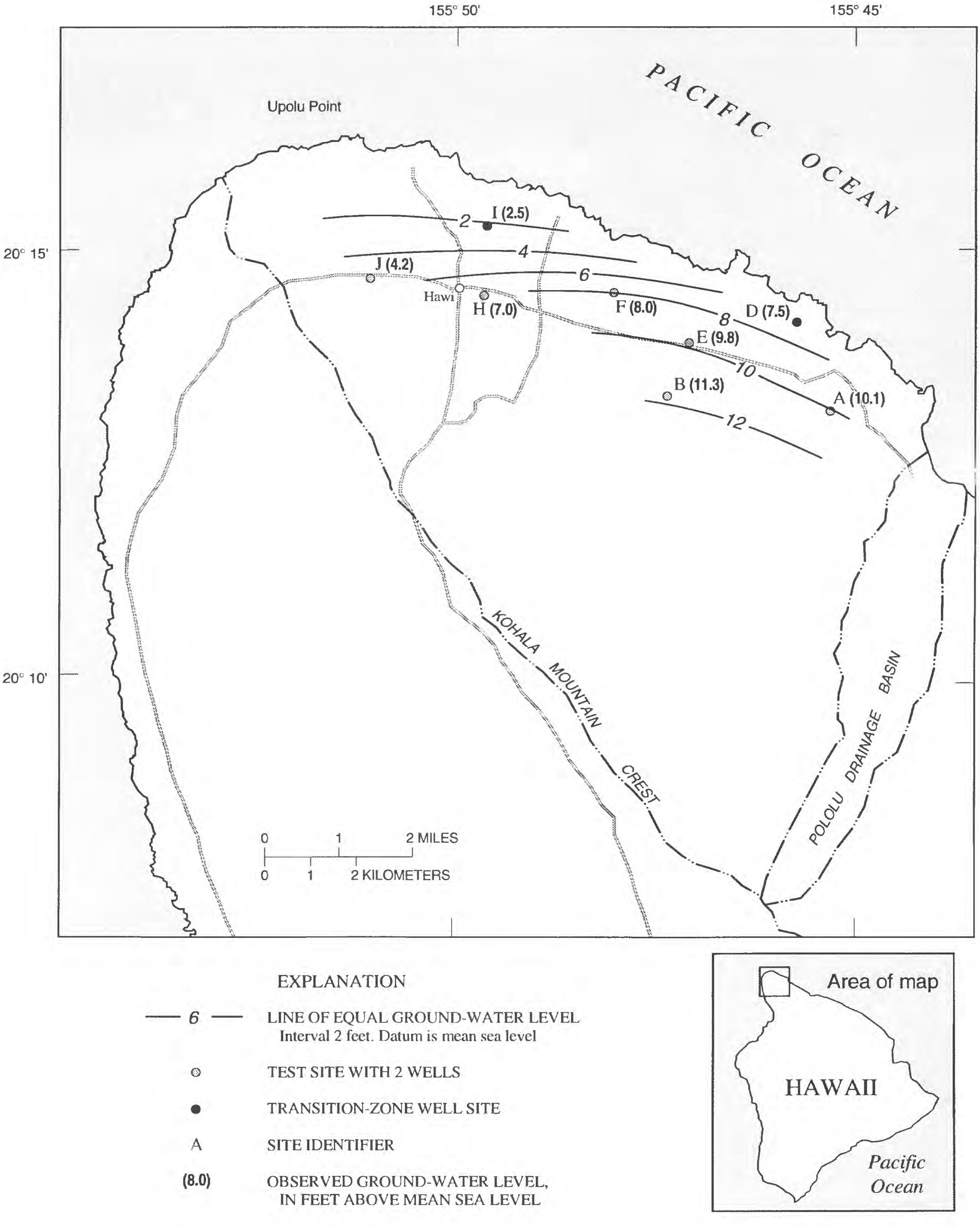

Figure 7. Observed ground-water levels in the Hawi basal aquifer and test-well sites, Kohala area, island of Hawaii.

Ground water discharges from the basal aquifer into the ocean and, near the shoreline, there is an upward component of ground-water flow. The upper 50 to 250 ft of the basaltic basal aquifer is largely decomposed by weathering, but it is not known if the weathered layer extends under the ocean. Waves along the coast may have eroded all or part of this layer. If a weathered layer exists, it would help impede the movement of ground water from the basal aquifer into the ocean because the hydraulic conductivity of weathered basalt is generally much lower than that of fresh basalt. Sedimentary deposits similar to those found along the shoreline of other islands in Hawaii are not present along the Kohala shoreline because of the relatively young age of the basalts in the area.

Springflow in the study area occurs primarily between 600 and 1,800 ft altitude and has been described by Stearns and Macdonald (1942) as perched water that, for the most part, issues from a clinker zone at the bottom of the Hawi Volcanics and above the red soil at the top of the Pololu Basalt.

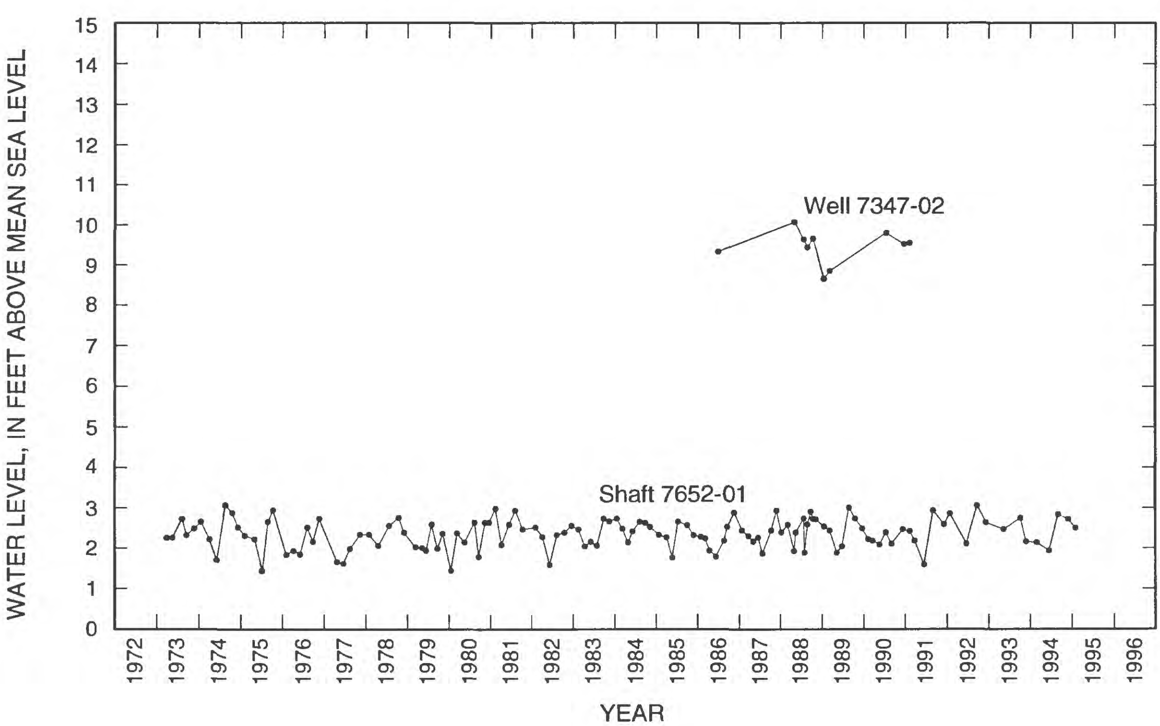

Figure 8. Water levels measured in well 7347-02 and shaft 7652-01, Kohala area, island of Hawaii.

Ground-Water Development

The locations of wells, shafts, and test holes constructed in the Hawi basal aquifer prior to this study are shown in figure 9. Altogether there are four wells, four shafts, and five test holes. With the exception of the DWS well (well 7449-02) near Hawi, all of the other wells, shafts, and test holes were drilled by sugar plantations. The first well (7448-01) was drilled in 1898 by the Kohala Sugar Company (State of Hawaii, 1970). Water from the well was used for sugar mill supply in 1901, but the well was ultimately abandoned (Davis and Yamanaga, 1963). Between 1899 and 1901 three shafts (Kohala, Alaalae, and Hoea) were sunk to sea level for water for sugarcane irrigation; a fourth shaft (Waikane) was constructed in 1920. Well 7347-02 was drilled in 1948 for domestic use and the Union Mill #1 well was drilled in 1965 with the intent of using the water for irrigating sugarcane. The wells were drilled at altitudes ranging from 310 to 540 ft. Finally, the five test holes described by Bowles and others (1974) were drilled in 1964. These holes were drilled at altitudes ranging from 170 to 362 ft. The shafts were constructed at low altitudes near the coast.

The present source of domestic water in the Kohala area comes primarily from the DWS well (0.6 Mgal/d) and three tunnel systems that have been dug to tap spring discharge: the Bond 1 tunnel, discharging at altitudes of about 1,000 ft and 1,400 ft; the Watt 1 tunnel, discharging at 1,700 and 1,800 ft; and the Murphy tunnel, discharging at about 1,250 ft. The greatest flows are from the Bond and Watt tunnel systems, which have discharges as large as 1.25 Mgal/d each. The Murphy tunnel discharges about 0.25 Mgal/d. The greatest untapped springflow is about 0.15 Mgal/d from the west branch of Halawa Gulch (fig. 4) (State of Hawaii, 1970). The total average flow for all tunnels and springs is 4 to 5 Mgal/d with a maximum total flow of 17 to 18 Mgal/d and a minimum total flow of about 1 Mgal/d (Stearns and Macdonald, 1946).

Sufficient data are not available to recreate the historical distribution and rates of ground-water development, although the general pattern of this development from 1940 to 1961 is discussed by Davis and Yamanaga (1963), and the pattern from 1962 through 1967 is available in State of Hawaii (1970). The following summarizes information in those two reports.

From 1940 through 1961 the average pumpage of ground-water from the aquifer was about 7.5 Mgal/d and most of the water was used to irrigate sugarcane (Davis and Yamanaga, 1963). The range in use during this time was 2.2 to 14.2 Mgal/d. Shaft pumpage from 1962 to 1967 was about 3.2 Mgal/d (State of Hawaii, 1970), about half of that from 1940 through 1961. Davis and Yamanaga (1963) indicated that chloride concentrations in one of the shafts averaged about 400 ppm and at another averaged about 1,500 ppm. Given that the shafts were constructed at low altitudes near the coast, and given their rate of pumpage, the relatively high chloride concentrations are to be expected. At the time of this study (1989-90) and as of 1995, the DWS well is the only well regularly pumped in the basal aquifer.

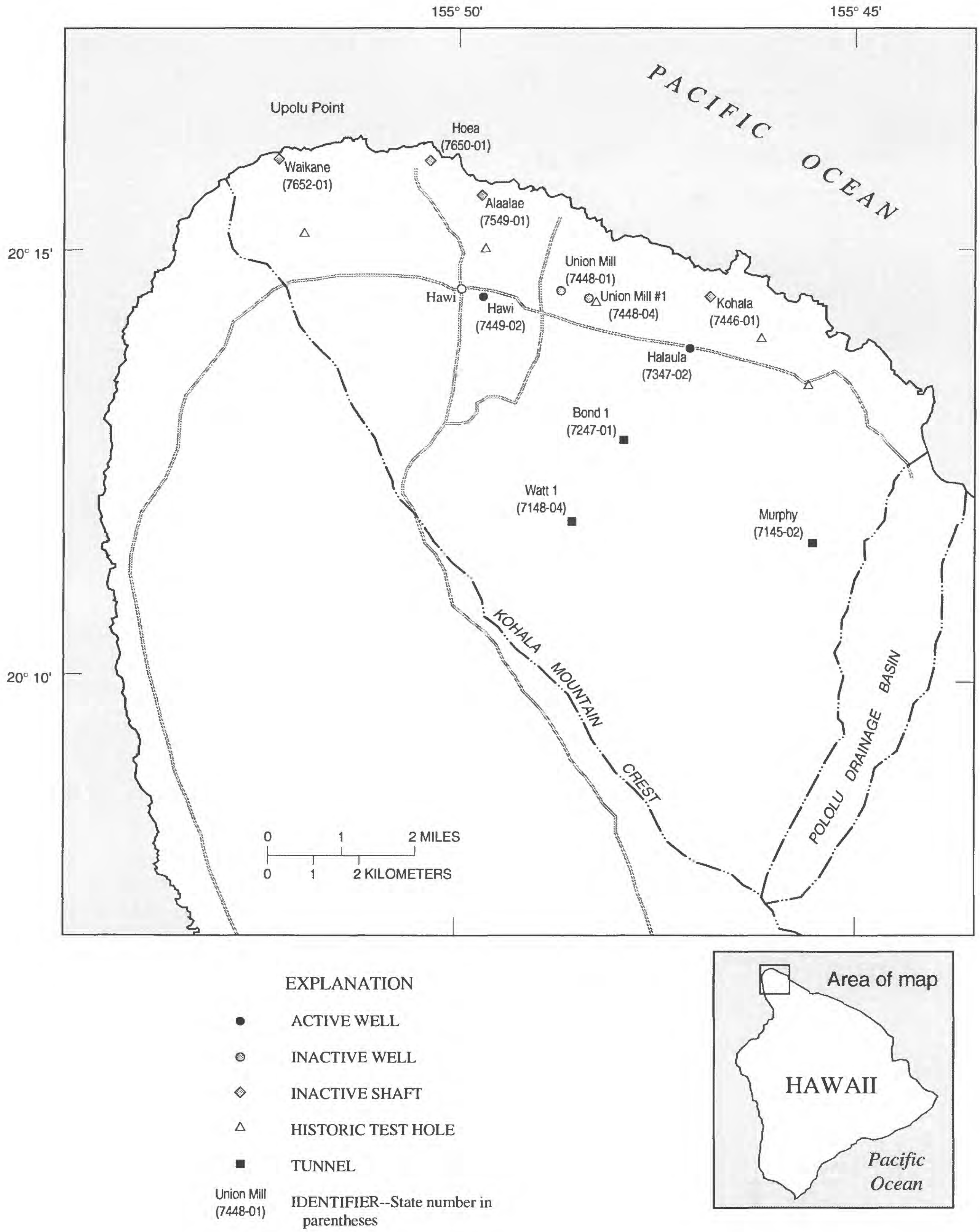

Figure 9. Locations of existing and historic wells, existing tunnels, and historic test holes in the Kohala area, island of Hawaii.

Ground-Water Quality

The quality of water in the basal aquifer was investigated by analyzing water samples from five of the eight test-well sites (A, B, E, F, and H in fig. 7) for concentrations of common ions. Samples were analyzed at the U.S. Geological Survey Central Laboratory according to standard methods (Fishman and Friedman, 1989, Wershaw, and others, 1987). Results show that the ground water in Kohala is typical of water from Hawaiian basalt aquifers (Swain, 1973). Dissolved ion concentrations were low, with specific conductance values ranging from 165 to 245 μS/cm and chloride concentrations ranging from 19 to 36 mg/L (table 1).

At three sites (A, B, and F), water samples were also collected for analysis for 18 dissolved metals and as many as 79 organic compounds, including agricultural chemicals, volatile constituents of fuel, and solvents (table 2). No dissolved metals or organic compounds were found at concentrations exceeding maximum contaminant levels (U.S. Environmental Protection Agency, 1991).

Iron and aluminum were the metals found in highest concentrations, as might be expected given their abundance in basalt. Iron and aluminum may also have been released into the water samples from the iron well casing, metal pump, and aluminum discharge line. The other metals were either not detected or detected at low (10 μg/L or less, except for barium) concentrations that are typical of ground water from basalt aquifers (Halbig and others, 1986; Eyre, 1994).

Samples were free of significant anthropogenic organic compounds. The only organic compounds reported were from well A, where toluene and xylene were found at or near the level of detection (0.2 μg/L). This concentration is far below the USEPA limit of 1,000 μg/L (U.S. Environmental Protection Agency, 1991). Given these low levels, it is possible that the presence of these compounds was the result of sample contamination during collection, false detection in the laboratory, or possible local contamination of the water during well drilling. Further sampling at this location would be necessary to verify the existence of the compounds.

Table 1. Concentrations of common ions and other water-quality characteristics of water samples from the Hawi basal aquifer, Kohala area, island of Hawaii
[mg/L, milligrams per liter; µg/L, micrograms per liter; <, value shown is less than actual value; µS/cm, microsiemens per centimeter at 25 °C]

State well number	7345-04	7449-02	7347-02	7448-07	7347-05
USGS test well (fig. 7)	A	H	E	F	B
Latitude	20°13′07″N	20°14′28″N	20°13′52″N	20°14′28″N	20°13′19″N
Longitude	155°45′20″W	155°49′42″W	155°47′06″W	155°48′02″W	155°47′23″W
Date	7/7/89	8/4/89	8/15/89	8/31/89	10/20/89
Time (24 hour)	1530	800	1510	1300	1400
Altitude of land surface (feet)	396	541	342	415	628
Depth of well, total (feet)	480	591	510	429	720
Flow rate, instantaneous (gallons per minute)	900	475	1,000	185	900
Specific conductance (µs/cm)	175	190	165	245	180
pH (standard units)	7	7.7	8	7.8	7.9
Temperature (°C)	21.5	22	22	24.5	22
Hardness, total (mg/L as $CaCO_3$)	56	44	45	58	47
Hardness noncarb. (mg/L as $CaCO_3$)	<1	<1	6	5	4
Calcium, dissolved (mg/L as Ca)	11	7.8	8.1	10	7.9
Magnesium, dissolved (mg/L as Mg)	6.9	5.9	6	7.9	6.5
Sodium, dissolved (mg/L as Na)	19	21	18	27	16
Potassium, dissolved (mg/L as K)	1.3	1.9	1.7	2.2	1.5
Alkalinity (mg/L as $CaCO_3$)	59	50	39	53	43
Sulfate, dissolved (mg/L as SO_4)	6	7	5	10	7
Chloride, dissolved (mg/L as Cl)	20	21	21	36	19
Fluoride, dissolved (mg/L as F)	0.1	<0.1	0.1	0.1	0.1
Silica, dissolved (mg/L as SiO_2)	37	51	41	44	44
Solids, sum of constituents, dissolved (mg/L)	138	148	18	174	133
Iron, dissolved (µg/L as Fe)	55	6	27	41	16
Manganese (µg/L as Mn)	<1	<1	1	6	<1

Table. 2. Concentrations of trace metal and organic compounds in water samples from the Hawi basal aquifer, Kohala area, island of Hawaii

[All values in micrograms per liter; <, actual value is less than value shown]

State well number	7345-04	7448-07	7347-05
USGS test site (fig. 7)	A	F	B
Date	7/7/89	8/31/89	10/20/89
Time	1530	1300	1400
Turbidity (NTU)	--	0.1	0.1
Dissolved metals			
Aluminum	130	10	<10
Arsenic	<1	<1	<1
Barium	100	<100	<100
Berylium	<10	<10	10
Cadmuim	<1	<1	<1
Chromium	2	1	1
Cobalt	1	1	1
Copper	4	4	2
Iron	180	50	40
Lead	2	4	1
Lithium	<10	<10	<10
Manganese	<10	<10	<10
Mercury	<0.1	0.1	<0.1
Molybdenum	<1	<1	<1
Nickel	6	<1	1
Selenium	<1	<1	<1
Silver	1	<1	<1
Zinc	<10	<10	<10
Organic compounds			
Alachlor	<0.1	<0.1	--
Aldrin	<0.01	<0.01	<0.01
Ametryne	<0.1	<0.1	--
Atrazine	<0.1	<0.1	--
Benzene	<0.2	<0.2	<0.2
Bromoform	<0.2	<0.2	<0.2
Carbontetrachloride	<0.2	<0.2	<0.2
Chlordane	<0.1	<0.1	<0.1
Chlorobenzene	<0.2	<0.2	<0.2
Chlorodibromomethane	<0.2	<0.2	<0.2
Chloroethane	<0.2	<0.2	<0.2
2-Chloroethylvinylether	<0.2	<0.2	<0.2
Chloroform	<0.2	<0.2	<0.2
Cyanazine	<0.1	<0.1	--
DDD	<0.01	<0.01	<0.01
DDE	<0.01	<0.01	<0.01
DDT	<0.01	<0.01	<0.01
DEF	--	<0.01	<0.01
Diazinon	<0.01	<0.01	<0.01
1,2-Dibromoethane	<0.2	<0.2	<0.2
Dichlorobromomethane	<0.2	<0.2	<0.2
1,2-Dichlorobenzene	<0.2	<0.2	<0.2
1,3-Dichlorobenzene	<0.2	<0.2	<0.2
1,4-Dichlorobenzene	<0.2	<0.2	<0.2
Dichlorodifluoromethane	<0.2	<0.2	<0.2
1, 2-Dichloroethane	<0.2	<0.2	<0.2
1,1-Dichloroethane	<0.2	<0.2	<0.2

Table. 2. Concentrations of trace metal and organic compounds in water samples from the Hawi basal aquifer, Kohala area, island of Hawaii--Continued
[All values in micrograms per liter; <, actual value is less than value shown]

Organic compounds--continued			
1,2-Transdichloroethene	<0.2	<0.2	<0.2
1,1-Dichloroethylene	<0.2	<0.2	<0.2
1,2-Dichloropropane	<0.2	<0.2	<0.2
1,3-Dichloropropene	<0.2	<0.2	<0.2
cis-1,3-Dichloropropene	<0.2	<0.2	<0.2
trans-1,3-Dichloropropene	<0.2	<0.2	<0.2
Dieldrin	<0.01	<0.01	<0.01
DiSyston	--	<0.01	<0.01
Endosulfan	<0.01	<0.01	<0.01
Endrin	<0.01	<0.01	<0.01
Ethion	<0.01	<0.01	<0.01
Ethylbenzene	<0.2	<0.2	<0.2
Heptachlor	<0.01	<0.01	<0.01
Heptachlorepoxide	<0.01	<0.01	<0.01
Lindane	<0.01	<0.01	<0.01
Malathion	<0.01	<0.01	<0.01
Methoxychlor	<0.01	<0.01	<0.01
Methylbromide	<0.20	<0.2	<0.2
Methylchloride	<0.20	<0.2	<0.2
Methylenechloride	<0.20	<0.2	<0.2
Methylparathion	<0.01	<0.01	<0.01
Methyltrithion	<0.01	<0.01	<0.01
Metolachlor	<0.1	<0.1	--
Metribuzin	<0.1	<0.1	--
Mirex	<0.01	<0.01	<0.01
Naphthalenes, polychlorinated	<0.1	<0.1	--
Parathion	<0.01	<0.01	<0.01
PCB	<0.1	<0.1	<0.1
Perthane	<0.1	<0.1	<0.1
Phorate	--	<0.01	<0.01
Prometon	<0.1	<0.1	--
Prometryne	<0.1	<0.1	--
Propazine	<0.1	<0.1	--
Silvex	<0.01	<0.01	--
Simazine	<0.1	<0.1	--
Simetryne	<0.1	<0.1	--
Styrene	<0.2	<0.2	<0.2
1,1,2,2-Tetrachloroethane	<0.2	<0.2	<0.2
Trichloroethylene	<0.2	<0.2	<0.2
Toluene	0.3	<0.2	<0.2
Trithion	<0.01	<0.01	--
Toxaphene	<1	<1	<1
1,1,1-Trichloroethane	<0.2	<0.2	<0.2
1,1,2-Trichloroethane	<0.2	<0.2	<0.2
Tetrachloroethylene	<0.2	<0.2	<0.2
Trichlorofluoromethane	<0.2	<0.2	<0.2
Trifluralin	<0.1	<0.1	--
Vinylchloride	<0.2	<0.2	<0.2
Xylene	0.2	<0.2	<0.2
2,4-D	<0.01	<0.01	--
2,4-DP	<0.01	<0.01	--
2,4,5-T	<0.01	<0.01	--

Vertical Extent of Freshwater

Saltwater underlies freshwater in the basal aquifer. When water is pumped from the basal aquifer, the lowering of ground-water levels associated with pumping will result in an upward movement of the saltwater. Ultimately, the amount of water that can be developed from the basal aquifer is constrained by the salinity of the water. To address the constraint on ground-water availability imposed by salinity, two wells (D and I, fig. 7) were designed to measure the vertical extent of freshwater and the upper part of the transition zone. Observation well D, located about 0.4 mi from the coast at an altitude of 108.5 ft, was completed at a depth of 351 ft below sea level. Observation well I, located about 0.7 mi from the coast at an altitude of 299.5 ft, was completed at a depth of 137 ft below sea level. The wells were open to the aquifer below the water table.

To estimate the thickness of freshwater and the upper transition zone, water samples were collected in March 1990 from several depths in each well and analyzed for chloride concentration (an indicator of salinity) (fig. 10). For this report, freshwater is defined as ground water containing water with a chloride concentration less than 250 mg/L (U.S. Environmental Protection Agency, 1991). Seawater collected around the Hawaiian islands has a chloride concentration of about 19,600 mg/L (Wentworth, 1939). The change in salinity between freshwater and seawater at depth is not abrupt, rather, freshwater and seawater mix and the change is somewhat gradual through a transition zone. The entire transition zone from freshwater to seawater includes all water with a chloride concentration between 250 mg/L and about 19,600 mg/L.

Through the transition zone, the density of the mixed water also varies from that of freshwater (about 1.000 gm/cm^3) to that of seawater (about 1.025 gm/cm^3). On the basis of this density difference, freshwater may be assumed to extend below sea level to a depth 40 times the water level above sea level. This is referred to as the Ghyben-Herzberg relation (Bear, 1979, p. 560). In practice, the depth defined by the Ghyben-Herzberg relation approximates the mid-point of the transition zone (Lau, 1962). The mid-point of the transition zone is at a chloride concentration of about 9,800 mg/L. Thus, the upper transition zone includes water with a chloride concentration between 250 and 9,800 mg/L.

In well D, the depth to a chloride concentration of 250 mg/L and thus the estimated thickness of freshwater is about 265 ft. The depth of the mid-point of the transition zone was about 345 ft below the water table, making the upper transition zone about 80 ft thick (fig. 10). In well I, the depth to a chloride concentration of 250 mg/L and thus the estimated thickness of freshwater is about 83 ft. No water samples were obtained at or below the mid-point of the transition zone in well I. On the basis of an extrapolation of the existing data, the depth of the mid-point of the transition zone was about 145 ft below the water table, making the thickness of the upper transition zone about 62 ft (fig. 10).

The preceding analysis is based on the assumption that the salinity profiles logged in the wells are representative of the salinity of water in the surrounding aquifer. However, each well is

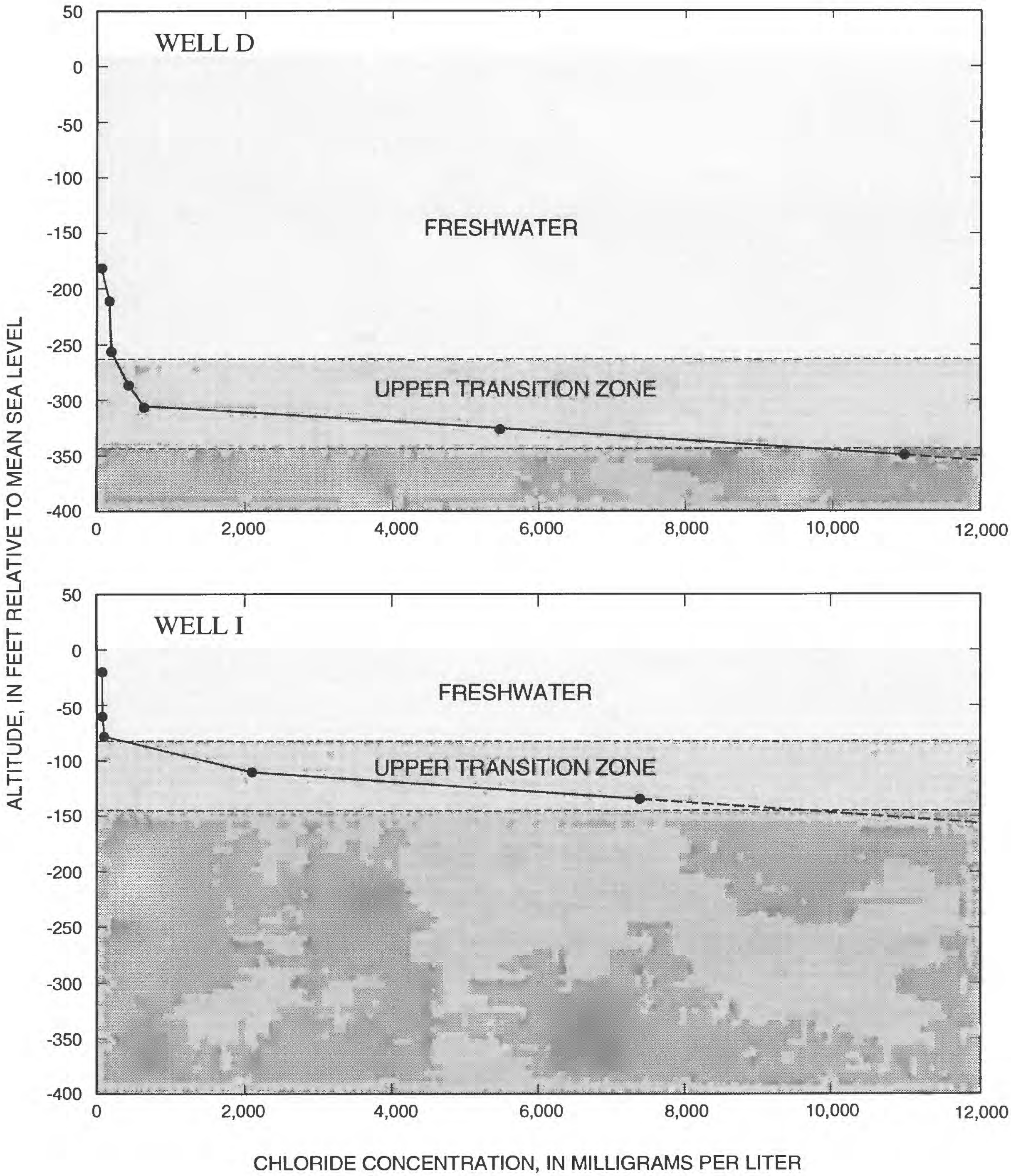

Figure 10. Chloride concentrations and depth for test wells D and I, Kohala area, island of Hawaii.

open to the aquifer for the entire depth below the water table, providing an open conduit through the pre-existing aquifer layers. If vertical hydraulic gradients exist in the aquifer, water will flow vertically within the well bore, entering from aquifer zones with greater hydraulic head and exiting to zones with lesser head. If ground-water flow in the aquifer is predominantly horizontal and vertical flow in the well bore is inconsequential, the salinity profile in the well can be expected to correspond closely to the salinity profile in the aquifer. However, vertical flow in the well could be of sufficient magnitude to distort the salinity profile and thickness of the transition zone in the well bore from that in the aquifer.

Test wells D and I are located between 0.4 and 0.7 mi from the shore, and here the dominant direction of ground-water movement is expected to be horizontal. As a result, vertical flow in the aquifer, and thus in the test wells would not be significant. If vertical flow does occur, it would most likely be upward because of the wells proximity to the shoreline where freshwater begins to discharge upward into the ocean. Upward flow within the well bore would tend to bring saltwater to higher altitudes in the well bore than exist in the aquifer. Accordingly, the salinity profile as logged in the well bore would be displaced upward by some unknown amount. Thus the well bore salinity profile would indicate that the top of the transition zone is shallower than it actually is in the aquifer.

HYDRAULIC CONDUCTIVITY OF THE BASAL AQUIFER

Estimates of the horizontal hydraulic conductivity of the basal aquifer were obtained from aquifer tests at five wells: A, E, F, H, and Union Mill #1 (fig. 11). Aquifer tests were done in wells drilled during the present study, and also in several wells drilled prior to this study. Similarly, aquifer-test data were mostly from tests done during the present study but also from data from several earlier tests (not done by USGS) that were reanalyzed as part of this study. A summary of well characteristics is shown in table 3.

Each test site consisted of a pumped well and an observation well. Each observation well was installed so that the depth of penetration into the aquifer was about the same as that of the corresponding pumped well. None of the wells fully penetrated the aquifer, the thickness of which is unknown. For an aquifer test, it is desirable to have the deepest possible well penetration that allows sufficient withdrawal without inducing an unacceptable saltwater upconing. As a result, the penetration of each pumped well drilled for this study is about one third of the estimated freshwater thickness, as approximated from the Ghyben-Herzberg relation. By avoiding the withdrawal of salty or brackish water, the complicating effects of variable-density fluid flow on hydraulic analysis were avoided.

Two types of aquifer tests were done at each site: a step-drawdown test and a 12-hour continuous pumping-rate test. The step-drawdown test involved measuring the drawdown induced in the pumped well at each of three to five successively higher pumping rates. Each step lasted about 1 hour. The sustained 12-hour test involved pumping the well at a steady rate for 12 hours and measuring the drawdown induced in both the pumped and the observation well over this time. Tests done during this study included step-drawdown tests at sites A, E, and F, and sustained pumping tests at site A, E, F, and H. Earlier tests included a step-drawdown test done in 1975 at site H by the County of Hawaii Department of Water Supply (unpub. data in files of U.S. Geological Survey, Honolulu), and a step-drawdown test and a sustained pumping test at Union Mill #1 in 1964 (Akinaka and others, 1975).

The step-drawdown data were analyzed to estimate the two components of drawdown in the pumped well: (1) the hydraulic head loss in the aquifer, (2) the hydraulic head loss from friction and turbulence within and near the well column, and (3) well entrance losses at the screen. An empirical relation between drawdown and pumping rate developed by Jacob (1947) allows a well efficiency at a desired pumping rate to be calculated. The measured drawdown in the well is then adjusted on the basis of the efficiency, and the resulting value represents the drawdown due only to hydraulic head loss in the aquifer. This adjusted value of drawdown is then used in subsequent equations of aquifer analysis.

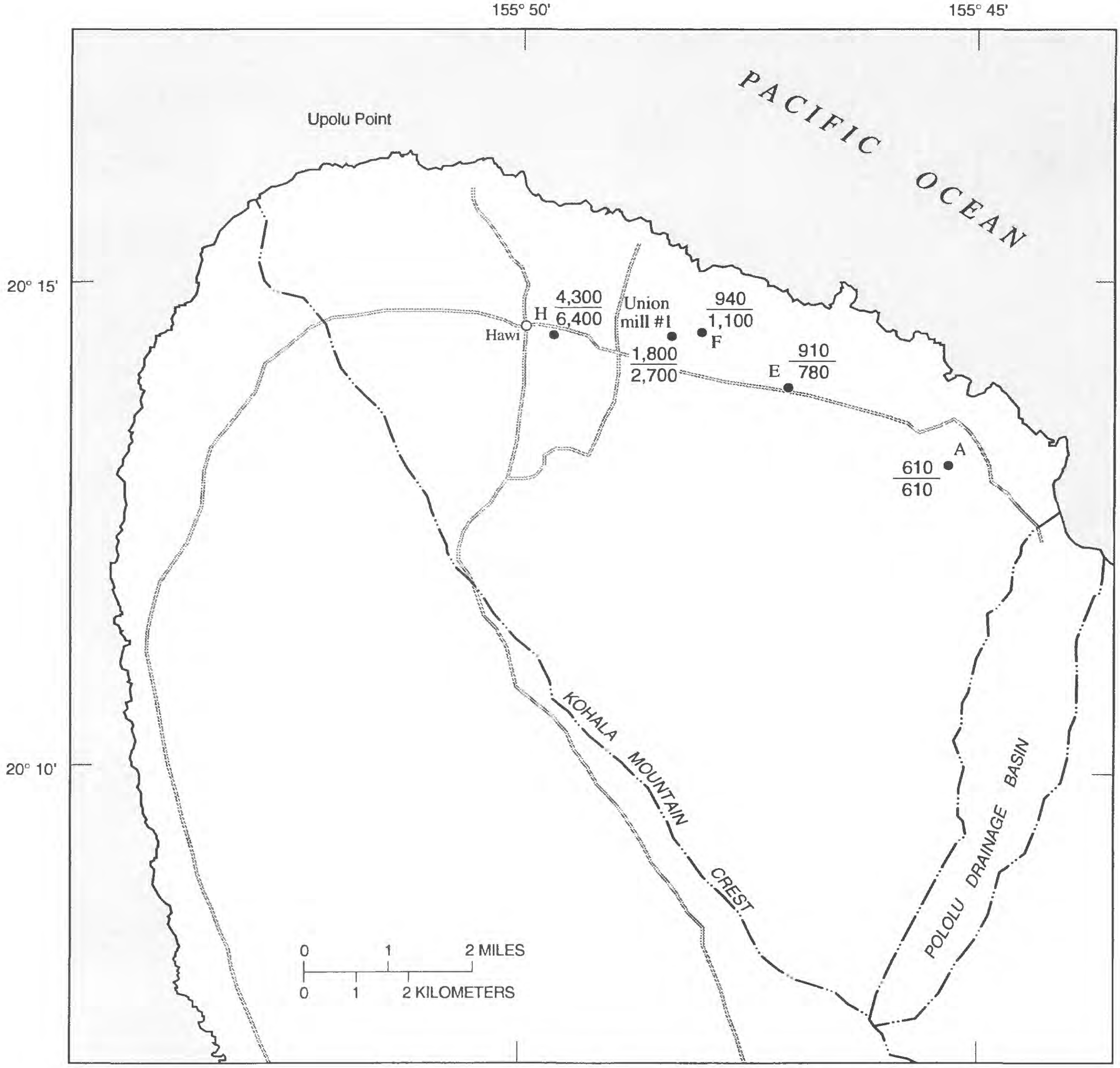

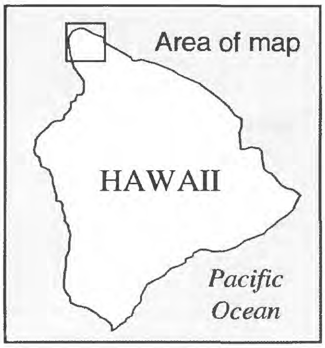

Figure 11. Aquifer-test values for horizontal hydraulic conductivity, Kohala area, island of Hawaii.

Table 3. Summary of characteristics of wells used for exploration and aquifer testing of the Hawi basal aquifer, Kohala area, island of Hawaii

[Includes exploratory wells drilled for this study and pre-existing wells used in the aquifer tests. Well number refers to the State of Hawaii numbering system. "Test pumping" wells were pumped during aquifer tests only and are not permanent withdrawal wells; --, no data]

Test site or well (figs. 7 and 11)	State well number	Well use	Land surface altitude (feet)	Depth drilled (feet)	Water-table altitude (feet)	Altitude of open interval (feet)	Type of open interval
A	7345-03	observation (water level)	395.3	440	10.2	175 to -45	open hole
A	7345-04	test pumping	395.9	495	10.3	-44 to -99	open hole
B	7347-04	observation (water level)	630.4	730	11.4	530 to -100	open hole
B	7347-05	test pumping	628.2	720	11.4	18 to -102	perforated steel/open hole
D	7445-01	observation (salinity profile)	108.5	460	7.5	74 to -352	open hole
E	7847-02	withdrawal	344	505	--	-8 to -161	open hole
E	7347-03	observation (water level)	340.5	405	9.8	261 to -64	open hole
F	7448-06	observation (water level)	411.6	440	8.0	289 to -28	open hole
F	7448-07	test pumping	414.8	429	8.1	8 to -22	steel perforated
H	7449-02	withdrawal	541.4	591	--	7 to -50	perforated steel/open hole
H	7449-03	observation (water level)	541.2	585	7.0	451 to -44	open hole
I	7549-03	observation (salinity profile)	299.5	436	2.3	169 to -137	open hole
J	7451-01	observation (water level)	566.6	632	4.2	467 to -65	open hole
J	7451-02	test pumping	566.8	632	4.8	7 to -65	perforated steel/open hole
Union Mill #1	7448-03	observation (water level)	306.3	402	4.9	306 to -96	open hole
Union Mill #1	7448-04	withdrawal	312	412	--	0 to -100	perforated steel/open hole

The adjusted drawdown data from the step-drawdown test were then analyzed using equation 1 (Harr, 1962; Polubarinova-Kochina, 1962):

$$K = \frac{Q\ln\left(1.6\frac{L}{r_w}\right)}{2\pi L s_w} \tag{1}$$

where: K is horizontal hydraulic conductivity, in feet per day;
Q is pumping rate, in cubic feet per day;
ln is natural logarithm (base e = 2.718);
L is length of the open interval of the well, in feet;
π is the number pi, equal to 3.1415;
r_w is radius of the well, in feet; and
s_w is drawdown in the pumped well, in feet, adjusted for well loss.

Equation 1 describes steady-state flow to a pumped well that partially penetrates an aquifer that is much thicker than the depth of the well, a condition met by the wells in this study. The geometry of flow is such that lines of equal drawdown in the aquifer take the shape of ellipses; thus the equation is referred to herein as the elliptical equation. This equation was solved for values of K using drawdown data from the step-drawdown tests, adjusted for well loss as described above.

Drawdown data from the 12-hour sustained pumping-rate tests were analyzed by the Thiem equation, which assumes steady, radial flow and requires measurements of drawdown in two observation wells. Differences in well construction required use of both the confined and unconfined forms of the Thiem equation (Todd, 1980):

$$K = \frac{Q\ln\left(\frac{r_2}{r_1}\right)}{2\pi b\,(s_1 - s_2)} \text{ (confined);} \tag{2}$$

and:

$$K = \frac{Q\ln\left(\frac{r_2}{r_1}\right)}{\pi\left(h_2^2 - h_1^2\right)} \text{ (unconfined),} \tag{3}$$

where: K is horizontal hydraulic conductivity, in feet per day;
Q is pumping rate, in cubic feet per day;
ln is natural logarithm (base e = 2.718);
r_1 is radial distance to observation well 1 (closer to the pumped well), in feet;
r_2 is radial distance to observation well 2, in feet;
π is the number pi, equal to 3.1415;
b is aquifer thickness, in feet;

s_1 is drawdown in observation well 1, in feet;
s_2 is drawdown in observation well 2, in feet;
h_1 is thickness of flow at observation well 1, in feet; and
h_2 is thickness of flow at observation well 2, in feet.

Several qualifications regarding application of the Thiem equation are pertinent. First, the pumped well was considered to be observation well 1, and the radius of the pumped well and the adjusted drawdown (computed from the step-drawdown analysis) were used. Next, because the thickness of the aquifer in the Kohala area is unknown, the submerged open length of the pumped well was substituted for aquifer thickness, b (flow is presumed to be horizontal and radial within the depth interval corresponding to the open length of the pumped well). The confined form of the Thiem equation was used for sites E, H, and Union Mill #1, sites where there was no drawdown-induced dewatering of the pumped interval because solid casings in the pumped wells extend below the level of drawdown. The unconfined form of the Thiem equation was used for sites A and F, sites where the pumped wells are open at the water table and drawdown caused dewatering of the pumped interval. Here, drawdown was subtracted from the pre-pumping submerged open length of the well to obtain the thickness of flow, h. Lastly, the Thiem equation assumes that steady-state, or equilibrium, flow has been attained. Typically, this constraint is closely approximated within a few hours in the permeable lavas of Hawaii at the short radial distances of these tests. Also relevant is the work of Bennett and others (1967), who conducted pumping tests in the Punjab region of West Pakistan. Using drawdown measurements in observation wells both within and outside the pumping interval, they demonstrated that the slope of the cone of depression within a few hundred feet of the pumped well stabilized after a few hours of pumping even though the cone of depression continued to expand. It was concluded that the flow to the pumped well was dominantly horizontal within the depth range of the open interval of the pumped well at radial distances of a few open-interval lengths, once the hydraulic gradient stabilized within this region. Consequently, the Thiem equation could be used to analyze this data.

Values of hydraulic conductivity(K) obtained from the aquifer tests ranged from 610 to 6,400 ft/day (table 4, fig. 11). Differences between values obtained by the two analytical methods at a given site ranged from 0 to 44 percent of the mean of the two values. Within the area of the tests (fig. 11), hydraulic conductivity seems to increase progressively in the northwest direction.

Table 4. Summary of aquifer-test data and results, Kohala area, island of Hawaii
[ft/d, feet per day; r, radius from center of pumped well; K, horizontal hydraulic conductivity of aquifer]

Test well site or well (fig. 11)	Pumped well	Length of pumping interval (feet)	Distance at observation well from pumped well (feet)	Step drawdown test		Sustained pumping test					
								Drawdown (feet)			
				Number of steps	K, calculated using elliptical equation (ft/d)	Pumping rate, Q (gal/min)	Duration of pumping (hours)	Observed in pumped well	Adjusted in pumped well	Observed in observation well	K, calculated using Theim equation, (ft/d)
A	7345-04	55	50	6	610	900	71	14.5	4.5	0.29	610
E	7347-02	153	40	5	910	1,240	14	7.5	1.6	0.31	780
F	7448-07	22	50	4	940	400	16	--	2.6	0.13	1,100
H	7449-02	57	55	4[a]	4,300	495	72	3.1	0.32	0.13	6,400
Union Mill #1[b]	7448-04	100	73	3	1,800	2,000	365	8.7	1.9	0.8	2,700
				$K_{average}$..............	1,700					$K_{average}$..............	2,300
				K_{median}..............	940					K_{median}..............	1,100

[a] Step-drawdown test was done at time of completion of well construction in 1975; data reported by Hawaii County Department of Water Supply (1975).
[b] Union mill #1 aquifer tests were done in 1965-66; data used in analysis reported in Akinaka and others (1975).

NUMERICAL SIMULATION OF THE BASAL AQUIFER

Ground-water flow in the basal aquifer was simulated using the two-dimensional areal ground-water model AQUIFEM-SALT (Voss, 1984), which is a finite-element numerical model that simulates an aquifer containing freshwater that floats on saltwater of greater density. The model simulates water-levels and movement of the freshwater only. The saltwater is assumed not to flow and to have a hydrostatic pressure distribution. It is assumed that the boundary between the freshwater and saltwater is a sharp interface and that the two waters do not mix. It is further assumed that the location of the interface in the model represents the mid-point of the transition zone of the aquifer. The position of the interface in the model is determined so that the hydrostatic pressure in both freshwater and saltwater are equal on both sides of the interface.

Description of the Model

Boundary conditions.--The inland extent of the basal aquifer terminates at the rift zones of Kohala Mountain. Although water moves through the rift zone into the basal aquifer, hydraulic conductivity of the dikes in the rift zone is orders of magnitude less than that of the basal aquifer. As a result, the rift zone was not included as part of the modeled area, but the discharge of water from it into the basal aquifer was accounted for in the model by specifying additional recharge to the model elements adjacent to the rift zone (fig. 12).

Discharge of ground water along the shoreline of the modeled area is simulated using a head-dependent flux boundary. Ground-water discharge into the ocean through the ocean floor occurs in model elements along of the shoreline (fig. 12). Such discharge occurs because there is a hydraulic connection between the basal aquifer and the ocean, and the freshwater head in the aquifer is higher than the head at the ocean floor. The rate at which water discharges is controlled by the difference between the freshwater head in the aquifer, the equivalent freshwater head at the ocean floor, and the thickness and vertical hydraulic conductivity of the basalt and the weathered zones in the basalt, if the latter exist on the ocean floor.

The model was extended beyond the primary study area to include the entire Pololu drainage area, because simulated pumpage in the Hawi basal aquifer was close to this area and drawdowns induced by pumping would be expected to extend into it and possibly beyond it. Because the geohydrologic setting of the area east of Pololu Stream is highly complex and not completely understood, the model was not extended into this area. Given the lack of detailed knowledge concerning the relation between the Waimanu basal aquifer and Pololu Stream, the stream was not simulated on the model. Model-simulated drawdowns at the mouth of Pololu Stream resulting from pumping 20 Mgal/d in the Hawi basal aquifer are discussed, however, in order to qualitatively evaluate the possible effect of pumping on this stream.

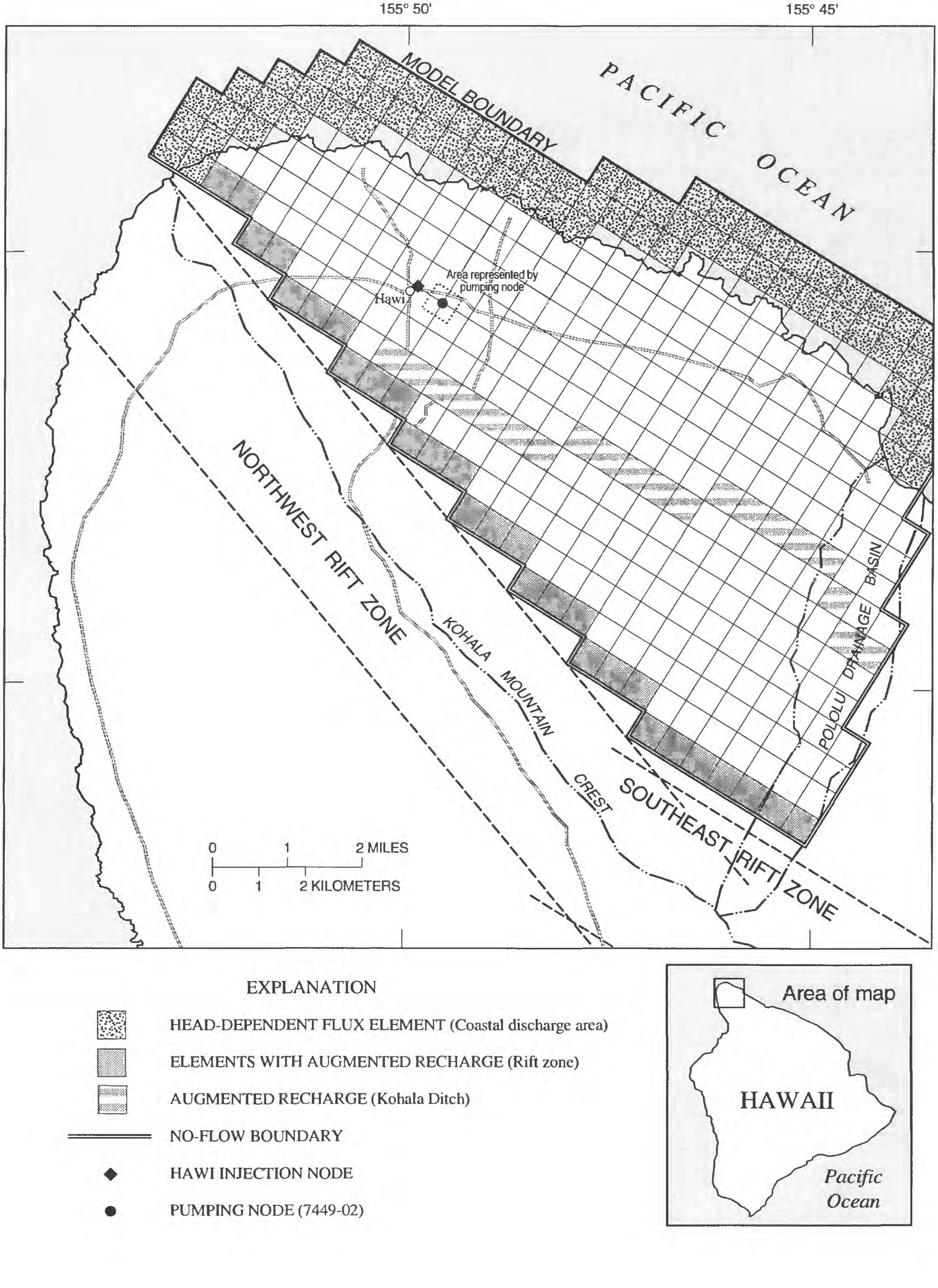

Figure 12. Model grid and boundaries used in the numerical simulation, Kohala area, island of Hawaii.

The basal aquifer is made up of hundreds of thin permeable lava flows that, because of subsidence of the island, now extend from the land surface to well below sea level. The depth of the bottom of the aquifer is not known. However, it is likely that the permeable lava flows extend several thousand feet below sea level because most Hawaiian volcanoes have subsided 6,000 to 12,000 ft (Moore, 1987). As a result, the model uses a single layer with a total thickness of 3,000 ft. This is not to indicate that freshwater extends to this depth. This depth represents only the estimated depth of permeable rock and conceptually, the total aquifer thickness includes both freshwater and saltwater. In the model, however, freshwater flows only in the interval between the water table and the freshwater-saltwater interface. The freshwater-saltwater interface as calculated by the model defines the bottom of the aquifer and is a no-flow boundary at a depth that is a function only of the local head in the aquifer.

Recharge.--Water is input into the model as ground-water recharge distributed areally over the modeled area using the distribution of mean annual recharge rates estimated by Shade (in press). Total recharge to the model is 78.4 Mgal/d. Recharge to the model from direct infiltration of rainfall on the basal aquifer, 60.3 Mgal/d, was distributed on the basis of values shown in figure 6. Recharge to the basal aquifer derived from that part of the rift zone between the topographic divide at the crest of Kohala Mountain and the boundary of the modeled area (8.1 Mgal/d) is accounted for by augmenting the recharge in the elements along the model boundary adjacent to the rift zone (fig. 12). Recharge to the basal aquifer from the Hawi hydroelectric plant injection wells (8 Mgal/d) was simulated as a constant flux to the model node where the injection wells are located. The estimated seepage loss from Kohala ditch (2 Mgal/d) was modeled as augmented recharge in elements along the ditch (fig. 12).

Ground-water pumpage.--The withdrawal of ground water at the DWS well (7449-02) was simulated as a constant rate of withdrawal equal to 0.6 Mgal/d. The location of the pumping node is shown in figure 12.

Hydraulic conductivity.--Values of hydraulic conductivity of the basal aquifer calculated during this study provided a range from 610 to 6,400 ft/d (table 4). The average value of hydraulic conductivity calculated from the aquifer test using the Thiem method is 2,300 ft/d; the median value is 1,100 ft/d. However, among the aquifer-test sites, higher values of hydraulic conductivity were obtained in the northwestern part of the basal aquifer than in the southeastern part (fig. 11). This variability was investigated and is discussed in the calibration section of the report. The hydraulic properties of the basal aquifer in Pololu Valley are not known, so that the hydraulic properties of the basal aquifer in this area were assumed to be the same as the southeastern part of the Hawi basal aquifer. In addition it is possible that the regular, tabular structure of basalt lava flows may cause the hydraulic conductivity to be greater along the lava flow direction than across it, making the aquifer areally anisotropic.

Shoreline discharge.--One of the most important considerations in boundary conditions is the nature of the discharge of freshwater from the basalt aquifer through the ocean floor. This discharge is impeded because, near the shoreline, ground-water movement is predominantly vertically upward and across the layering of the basalt flows. There is resistance to vertical movement because the freshwater must flow through the dense, less permeable interior part of individual lava flows. There would be additional resistance to vertical movement if the basalt layers are weathered or there are ocean bottom sediments overlying the basalt. Also, freshwater must discharge against the saltwater head at the ocean floor. In the model, the saltwater head would be expressed as an equivalent freshwater head, $h_f = (1.025z - z)$ for z equal to the depth below sea level to the ocean floor. Because AQUIFEM-SALT does not distinguish between freshwater and saltwater, the model will use the ocean as a source of freshwater to the aquifer if the calculated freshwater equivalent head at the ocean floor in the discharge area of the model (fig. 12) exceeds the head in the underlying basalt aquifer. To avoid this, the freshwater equivalent head of the ocean was set to zero in the discharge area. Thus, in any simulation, the aquifer head would be greater than the head at the modeled discharge area. The effect on the simulation is a small error in the simulated hydraulic connection between the ocean and the basal aquifer. This error would tend to make the model overestimate water-level declines associated with pumpage and thus make the model more conservative when estimating ground-water availability.

Near the shoreline, ground water moves upward from the basal aquifer to discharge into the ocean. This movement is resisted by the vertical hydraulic conductivity (K') of the basalts and by the weathered zone at the top of the basalt if it exists. Discharge is proportional to the effective vertical hydraulic conductivity of the basalt and weathered zone (assuming it exists) divided by the thickness of the zone of discharge (m'). As discussed previously, the vertical hydraulic conductivity of basalts in Hawaii is assumed to fall within a range of about one tenth to one thousandth of the horizontal hydraulic conductivity. On the basis of results of the aquifer tests for the Hawi basal aquifer, this would result in a range of values for the vertical hydraulic conductivity of the basalt between 0.6 to 640 ft/d. The thickness of the zone of discharge can be approximated by estimating the freshwater thickness at the shoreline. Water levels near the shoreline are about 5 ft, indicating a freshwater thickness of about 200 ft. For modeling purposes, it can be assumed the vertical distance over which discharge occurs is one-half this distance, or 100 ft. Assuming that the weathered zone does not exist, the value for K'/m' would fall between 0.006 and 6.4 ft/d/d (d^{-1}). The ratio K'/m' is referred to as the hydraulic connection between the basal aquifer and the ocean.

Calibration of the Steady-State Model

The model was calibrated by comparison of model-calculated water levels with water levels measured in the basal aquifer at the test wells (fig. 7) on March 22, 1990. Two parameters were varied during the calibration procedure; the horizontal hydraulic conductivity, *K*, of the basal aquifer, and the hydraulic connection of the basal aquifer with the ocean *(K'/m')*. Despite being varied, the simulated values for the horizontal hydraulic conductivity of the aquifer were kept within the general range of values obtained from the aquifer tests and ultimately varied spatially in the same manner as indicated by the test results. Thus, the major uncertainty in modeled parameters was the hydraulic connection of the aquifer with the ocean.

The first step in the calibration analysis was to make a series of simulations where the simulated *K* was held constant while the simulated value of *K'/m'* was varied over a range from 0.0005 to 10.0 ft/d/ft. The model was run to steady state for each value of *K'/m'*, and the values of model-calculated water levels at the test wells were recorded. Three sets of simulations were made using simulated values for *K* of 500; 1,000; and 5,000 ft/d. Results of this series of simulations are shown in figure 13.

The relation between the model-calculated water levels and water levels observed at the test wells varied spatially, falling into two groups (fig. 13). The plot of model-calculated water levels compared with the simulated value of *K'/m'* shown for test well E (fig. 13) is representative for wells E, A B, D, and F, all of which are located in the eastern part of the basal aquifer. A similar plot for test well H (fig. 13) is representative for wells H, I, and J, all of which are in the western part of the basal aquifer.

As shown in figure 13, it was possible to match water levels observed at test wells E, A, B, D, and F for all simulated values of *K*, although the value for *K'/m'* ranged from about 0.004 to 0.1 ft/d/ft. On the other hand, as shown in figure 13, values of *K* greater than 1,000 ft/d are necessary in order to match water levels observed in test holes H, I, and J regardless of the simulated value for *K'/m'*. At test well H, a match between model-calculated and observed water levels was obtained for *K* equal to 5,000 ft/d and the *K'/m'* equal to about 0.006 ft/d/ft.

Several conclusions are possible from the above information. First, larger values for *K* are required in the model for the western part of the basal aquifer compared with the eastern part. This corresponds to the distribution of hydraulic conductivity indicated by the aquifer tests. Second, the range in values of *K'/m'* that resulted in model-calculated water levels matching observed (0.004 to 0.1 ft/d/ft) are within the general range of values previously calculated for this parameter (0.006 to 6.4 ft/d/ft) assuming vertical movement of ground water is resisted only by the vertical hydraulic conductivity (*K'*) of the basalt flows.

The spatial variability of *K* of the basal aquifer necessary to allow a closer match between model-calculated and observed water levels was investigated further, initially by using the results

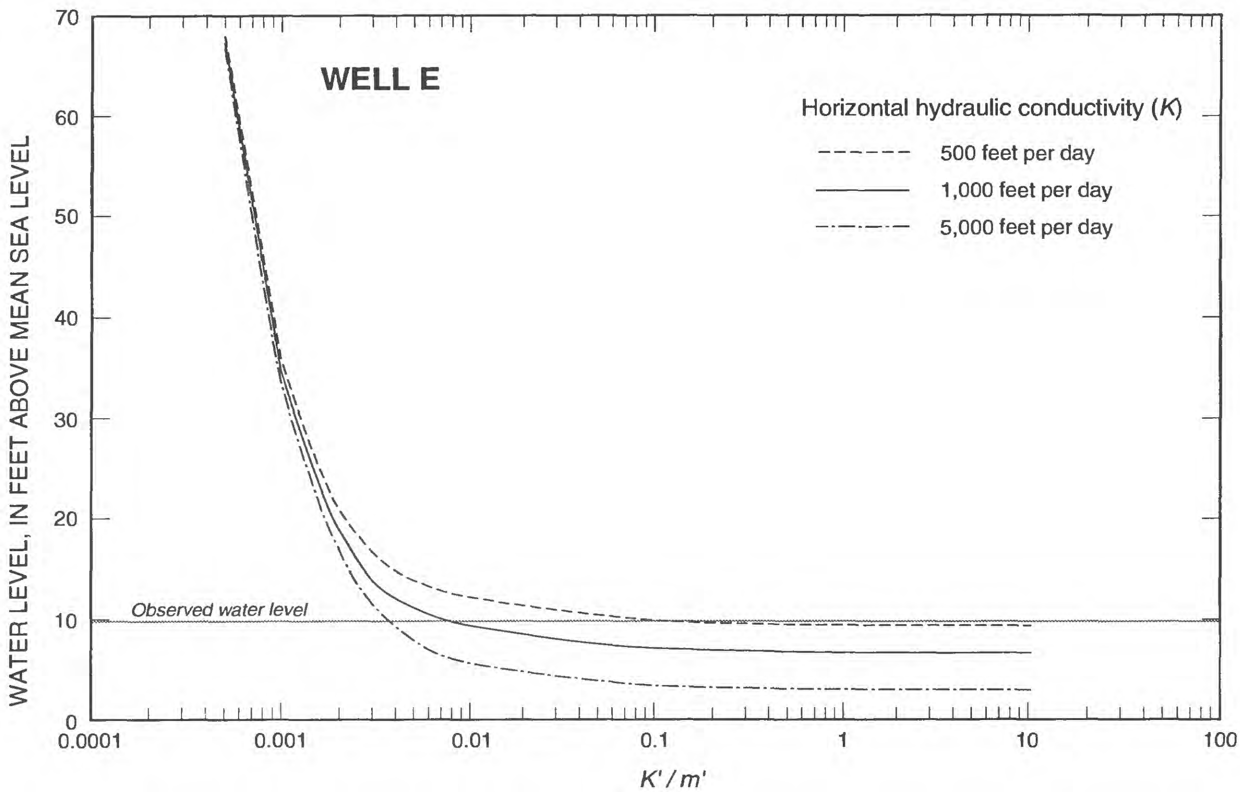

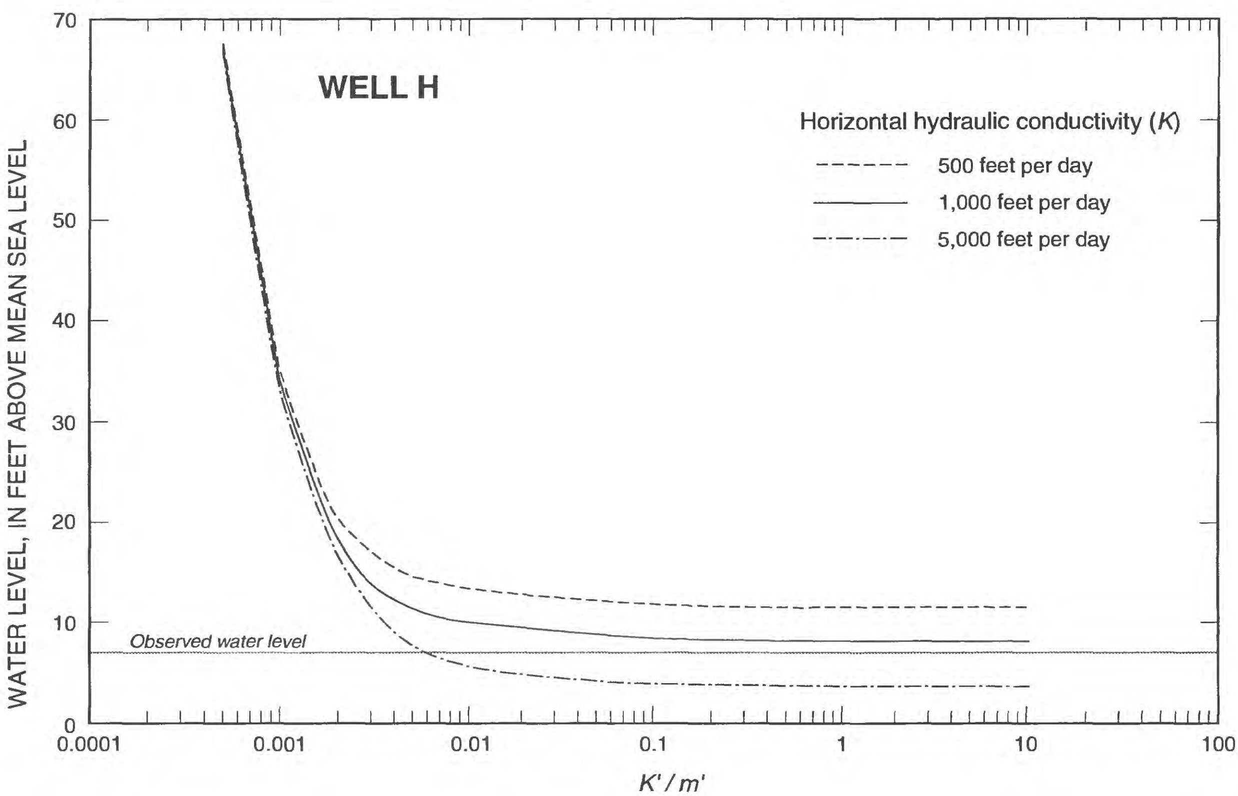

Figure 13. Model-calculated water levels at test wells E and H, for selected values of horizontal hydraulic conductivity and hydraulic connection, *K' / m'*, between the basal aquifer and the ocean, Kohala area, island of Hawaii (location of wells shown in figure 7).

of three of the model simulations from the initial series. These three simulations used a value for K of 500; 1,000; and 5,000 ft/d and a value for K'/m' equal to 0.01 ft/d/ft. Model-calculated and observed water levels were plotted on a scatter diagram (fig. 14*A*). The scatter diagram indicates any bias or trends in model-calculated water levels, such as all of the model-calculated water levels being higher or lower than observed.

The simulated value for K'/m' used for the above models (0.01 ft/d/ft) was selected for several reasons. First, as shown in figure 13, model-calculated water levels for all the wells are relatively insensitive to values of K'/m' greater than about 0.1 ft/d/ft, and model-calculated water levels become sensitive to values lower than 0.1 ft/d/ft. The model becomes increasingly sensitive to values of K'/m' less than about 0.01 ft/d/ft and for values lower than about 0.004 ft/d/ft, model-calculated water levels rise sharply beyond observed water levels for all values of simulated K. Second, when pumping is simulated, lower values of K'/m' result in greater model-simulated drawdowns and freshwater-saltwater interface rise for a given distribution and rate of ground-water pumpage, other things being equal. Therefore, for lower values of K'/m', the model becomes more conservative for estimation of ground-water availability. Finally, the value used for this analysis (0.01 ft/d/ft) also fell within the range of values (0.004 to 0.1 ft/d/ft) that resulted in model-calculated water levels matching observed water levels.

As expected, these simulations did not produce an acceptable match to observed water levels. For K equal to 500 ft/d, all of the model-calculated water levels were significantly higher than observed water levels. For K equal to 1,000 ft/d, a strong bias existed in the distribution of water levels; model-calculated water levels were significantly higher than observed on the western side of the aquifer (wells I, J, and H; fig. 14*A*) and very close to observed water levels on the eastern side (wells E, F, D, A, and B). For K equal to 5,000 ft/d, model-calculated water levels were somewhat higher than observed on the western side of the aquifer and significantly lower than observed on the eastern side. These trends in the model-calculated water levels indicate that to match observed water levels a relatively low K is required in the eastern part of the model and a relatively high K is required in the western part.

On the basis of the above analyses, the value of K of the aquifer was then varied spatially on the model with higher values in the western part of the model and lower values on the eastern part of the aquifer while K'/m' was held constant at 0.01 ft/d/ft. Various ranges and distributions of K (ranging from 250 to 8,000 ft/d across the model) were tested and nearly all of these simulations improved the model. The best match in this series of simulations resulted in a model with K varying from 650 to 5,000 ft/d (fig. 14*B*). The average difference between model-calculated and observed water levels for this distribution was 0.8 ft. Water levels calculated by the model were still relatively high at test wells I and J. To improve the match, K'/m' was increased from 0.01 to 0.1 ft/d/ft in the western part of the model (fig. 15); this resulted in a much better fit between model-calculated and observed water levels (fig. 14*B*). The average difference between model-calculated

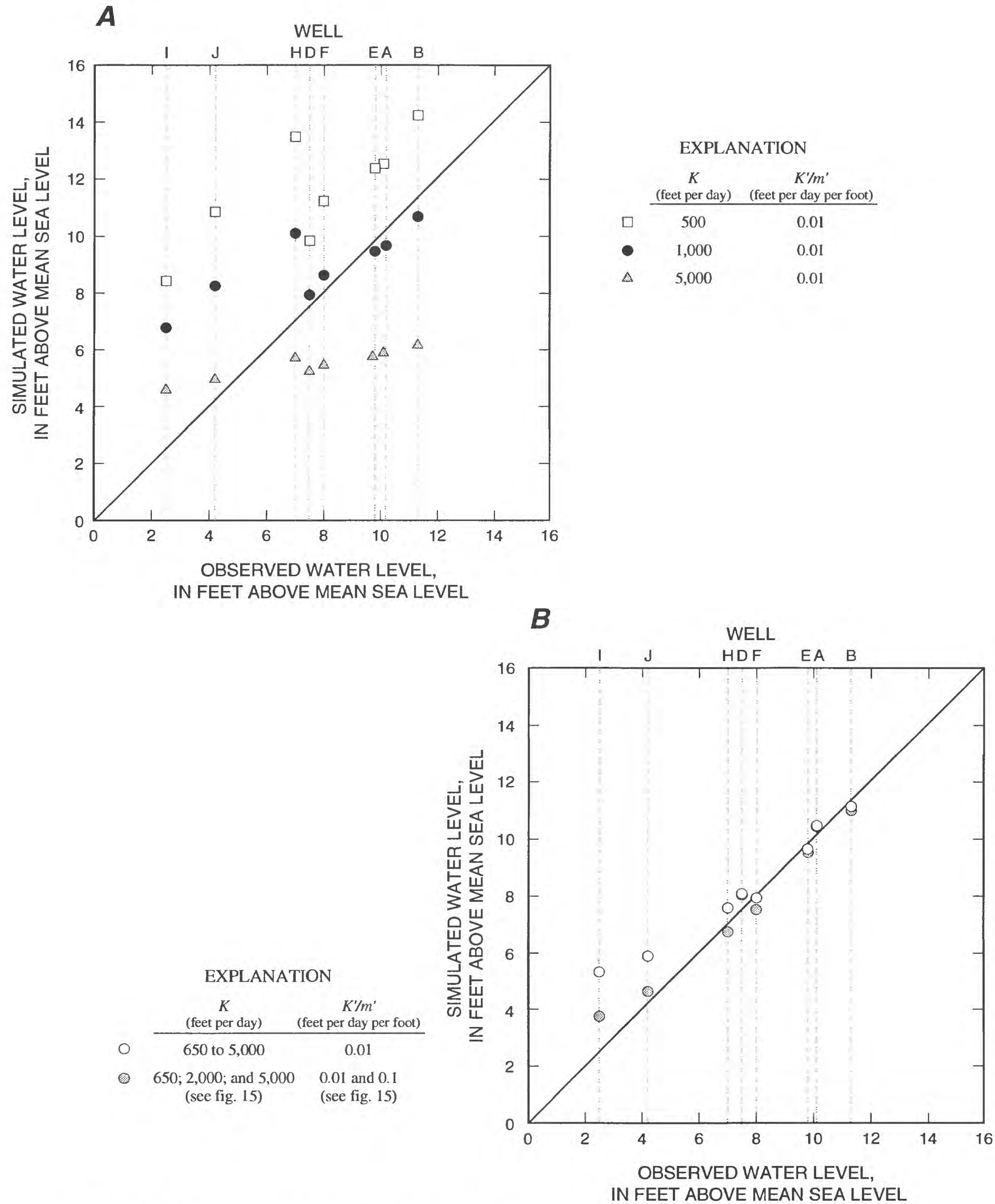

Figure 14. Model-calculated water levels and observed water levels for selected values of horizontal hydraulic conductivity (*K*) and the hydraulic connection between aquifer and ocean (*K'/m'*), Kohala area, island of Hawaii.

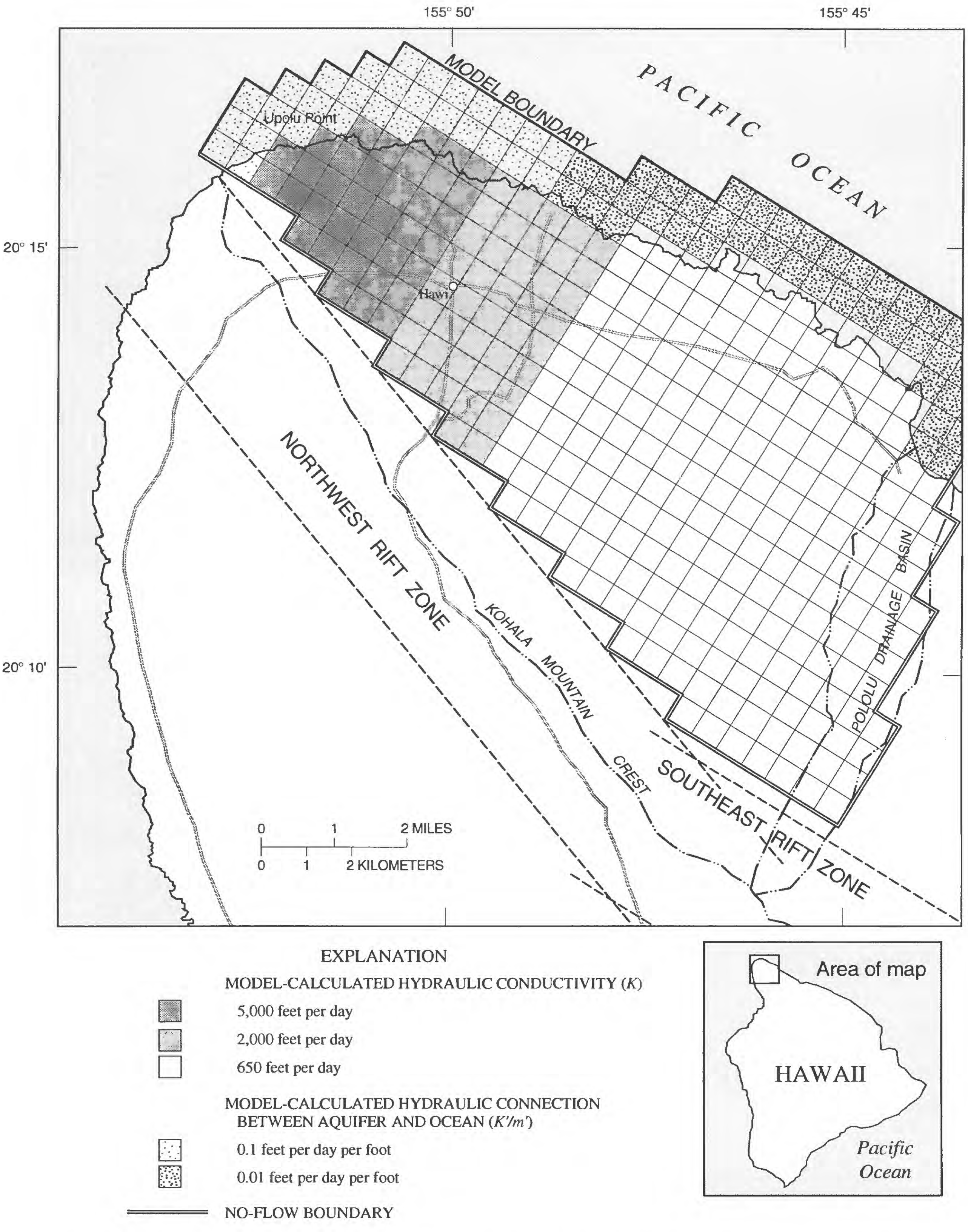

Figure 15. Distribution of horizontal hydraulic conductivity and hydraulic connection between the aquifer and ocean as modeled, Kohala area, island of Hawaii.

and observed water levels was about 0.5 ft and this version of the model was accepted as the best representation of the aquifer based on available data. Increasing *K'/m'* in the western part of the model was believed to be justified because of the higher value of *K* of this area as compared with the eastern part of the model. Model-calculated water-levels were compared with those from field data and are shown in figure 16. Model-calculated depth of the freshwater-saltwater interface is shown in figure 17.

The sources and discharges characterizing the steady-state simulation described above are summarized in table 5. The magnitude of the flow components shown in the table represent mean annual conditions. Shade (in press) has shown that these conditions vary significantly during an average year, but even so, the time response of the aquifer, in terms of changes in water levels is small (1 ft or less) relative to seasonal changes in the magnitude of the individual components of the water budget.

Table 5. Steady-state ground-water budget (existing pumpage) for the numerical model, Kohala area, island of Hawaii

Ground-water sources		Million gallons per day
Direct infiltration of precipitation		60.3
High-level discharge into the basal aquifer		8.1
Kohala ditch seepage		2.0
Hydroelectric plant injection wells		8.0
	Total..........	78.4
Ground-water discharges		
Into ocean		77.8
Existing pumpage		0.6
	Total..........	78.4

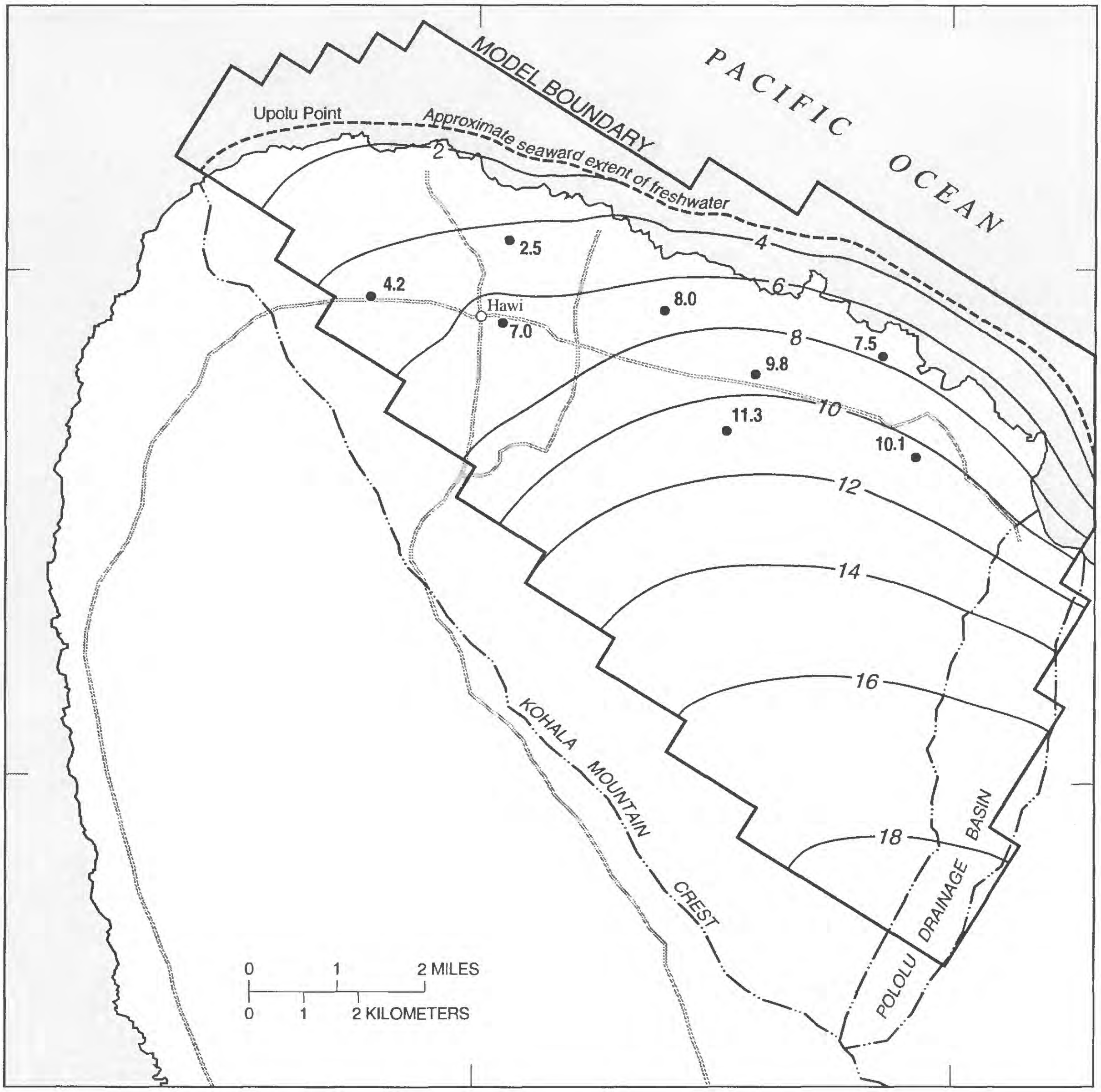

EXPLANATION

6 LINE OF EQUAL MODEL-CALCULATED GROUND-WATER LEVEL--Interval 2 feet. Datum is mean sea level

10.1 • WELL LOCATION AND OBSERVED GROUND-WATER LEVEL, IN FEET ABOVE MEAN SEA LEVEL

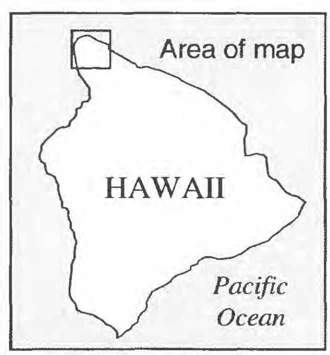

Figure 16. Model-calculated and observed ground-water levels, Kohala area, island of Hawaii.

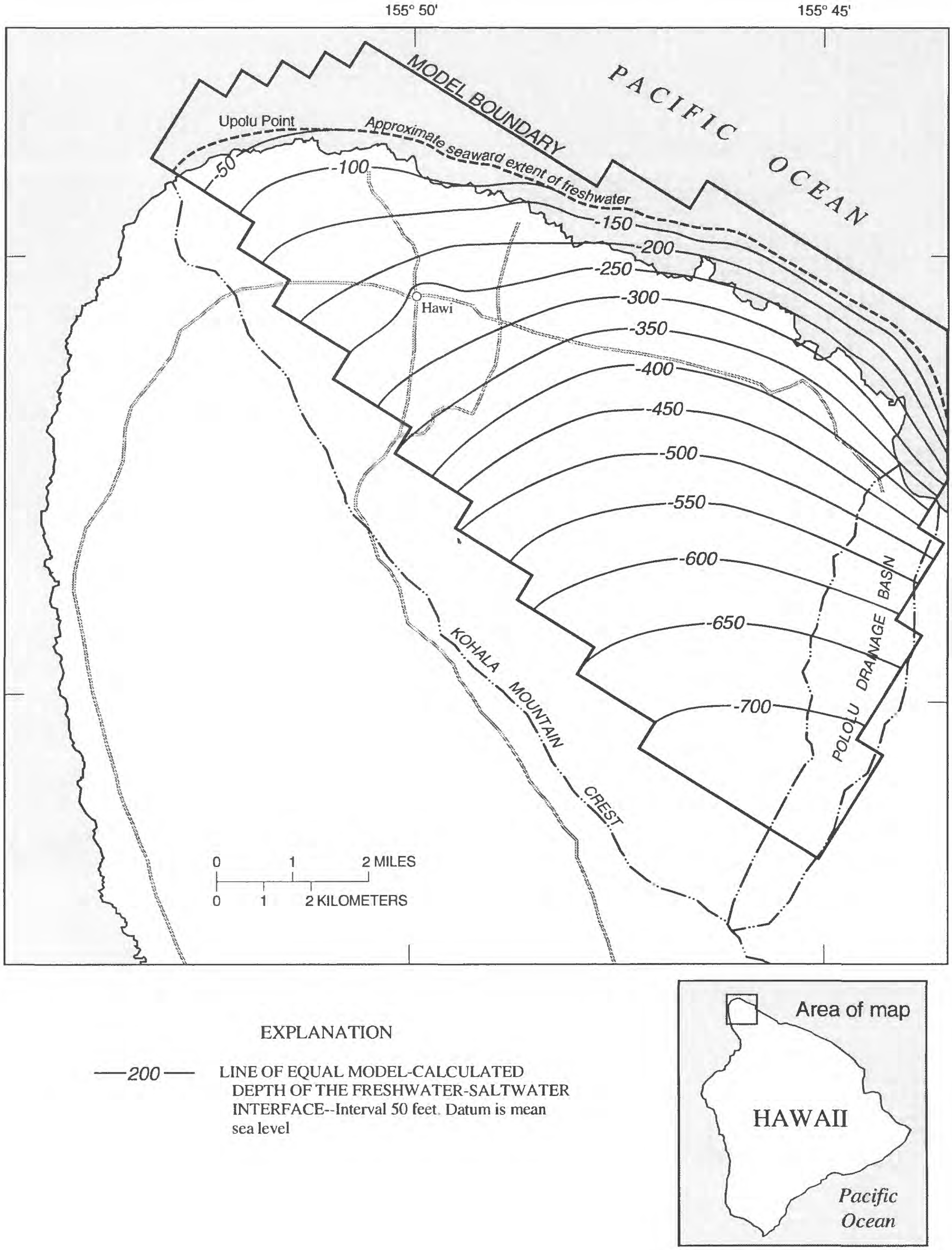

EXPLANATION

—200— LINE OF EQUAL MODEL-CALCULATED DEPTH OF THE FRESHWATER-SALTWATER INTERFACE--Interval 50 feet. Datum is mean sea level

Figure 17. Model-calculated depth of the freshwater-saltwater interface, Kohala area, island of Hawaii.

Response of the Basal Aquifer to Ground-Water Pumping

The response of the basal aquifer to pumping 20 Mgal/d above that currently being withdrawn from the aquifer was simulated for two pumping scenarios. In each scenario, there are six pumping sites aligned roughly parallel to the coast, with the four inside sites each pumping 4 Mgal/d and two outside sites each pumping 2 Mgal/d. The location of pumping sites and pumping rates are shown in figure 18. The only difference between the two scenarios is the areal distribution of pumping. In the first scenario, the six pumping sites were located over a distance of 5 mi with the four sites pumping 4 Mgal/d in the middle 3 mi. In the second scenario, the six pumping sites were located over a distance of 3 mi with the four sites pumping 4 Mgal/d concentrated in the middle 1.5 mi. In general, the simulations show that increasing ground-water pumping results in (1) a decrease of discharge to coastal discharge boundary equal to the amount of pumpage (see tables 5 and 7); (2) a decline in water-table altitude (see figs.19 and 20); and (3) a decrease in the depth to the freshwater-saltwater interface (see figs. 17, 21, and 22).

In analyzing the model results in terms of water-level declines and the resulting rise in the freshwater-saltwater interface, a distinction needs to be made between model-calculated drawdown for a model node and the actual drawdown that would occur in a well or wells. The model-calculated drawdown represents the average drawdown in an area around the model node (see fig. 12) and in all cases drawdown in a well or wells will be greater. The actual difference between the two will depend on the number of wells that the withdrawal in a given node represents, the pumping rate of individual wells, and the construction details of the well. The model assumes full penetration of the pumped well and for a pumping rate of 1.0 Mgal/d per well, application of an equation developed by Prickett (1967) indicates that drawdown in a well would be about 0.3 ft greater than the model-calculated drawdown at a node. Wells in basal aquifers are typically constructed to depth ranging from 50 to 200 ft below sea level rather than penetrating the entire freshwater thickness of the aquifer, however, and the effects of partial penetration would increase actual drawdown in a well above values calculated from Prickett's equation. These considerations indicate that the model cannot directly address the subject of individual well yields compared with well depth and that this information must be gained from actual field experience or from more detailed "local scale" model analysis.

Model-calculated changes in water level.--The decline in ground-water levels estimated by the model for scenarios 1 and 2 are shown in figures 19 and 20, respectively. Water-level declines for the first scenario range from about 1 to 3.5 ft at the pumping centers and to about 0.1 ft near the extreme northwestern edge of the model. Water-level declines in the extended study area are about 1 ft.

Water-level declines for the second model scenario are similar to those of scenario 1 except that drawdown at the pumping centers ranges from about 2 to almost 5 ft, an increase of as much as 1.5 ft over the first scenario. The increase in drawdown is a result of more localized pumping.

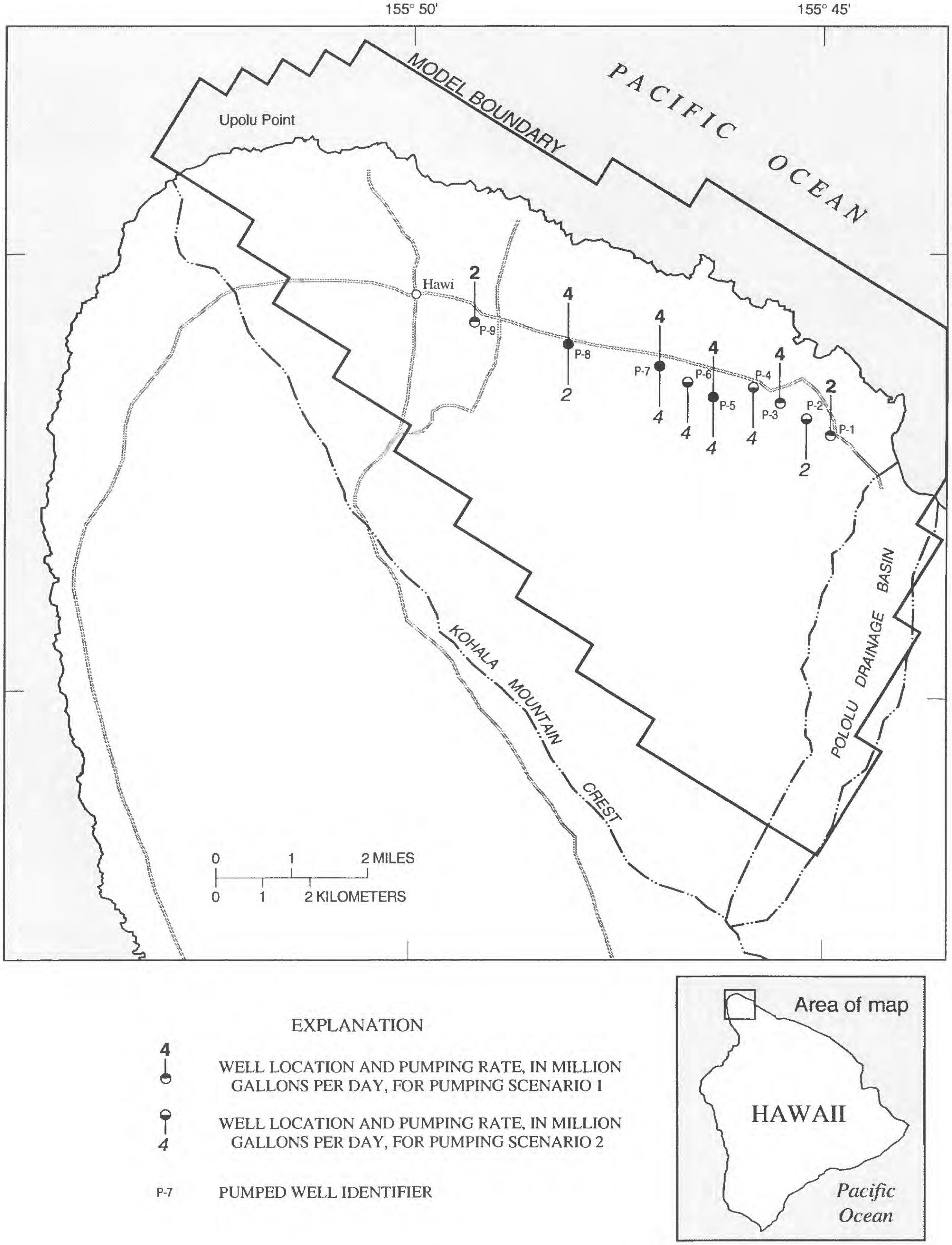

Figure 18. Pumping rates used for the two simulated pumping scenarios, Kohala area, island of Hawaii.

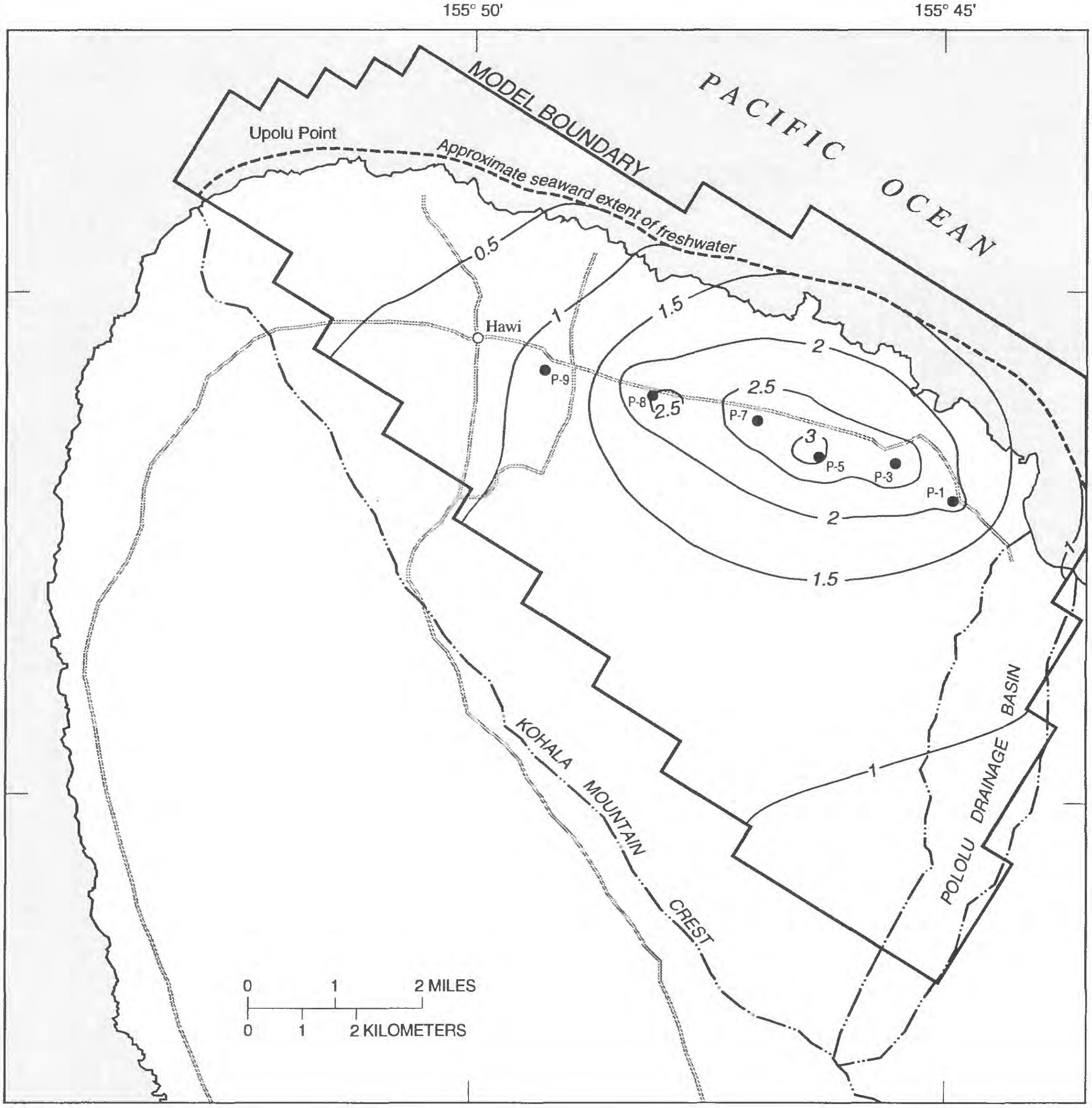

EXPLANATION

—3— LINE OF EQUAL MODEL-CALCULATED DRAWDOWN--Interval 0.5 feet

P-7 ● PUMPED WELL AND IDENTIFIER

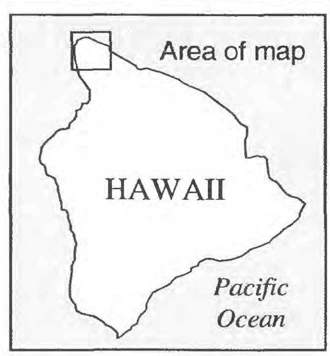

Figure 19. Model-calculated drawdown for pumping scenario 1, Kohala area, island of Hawaii.

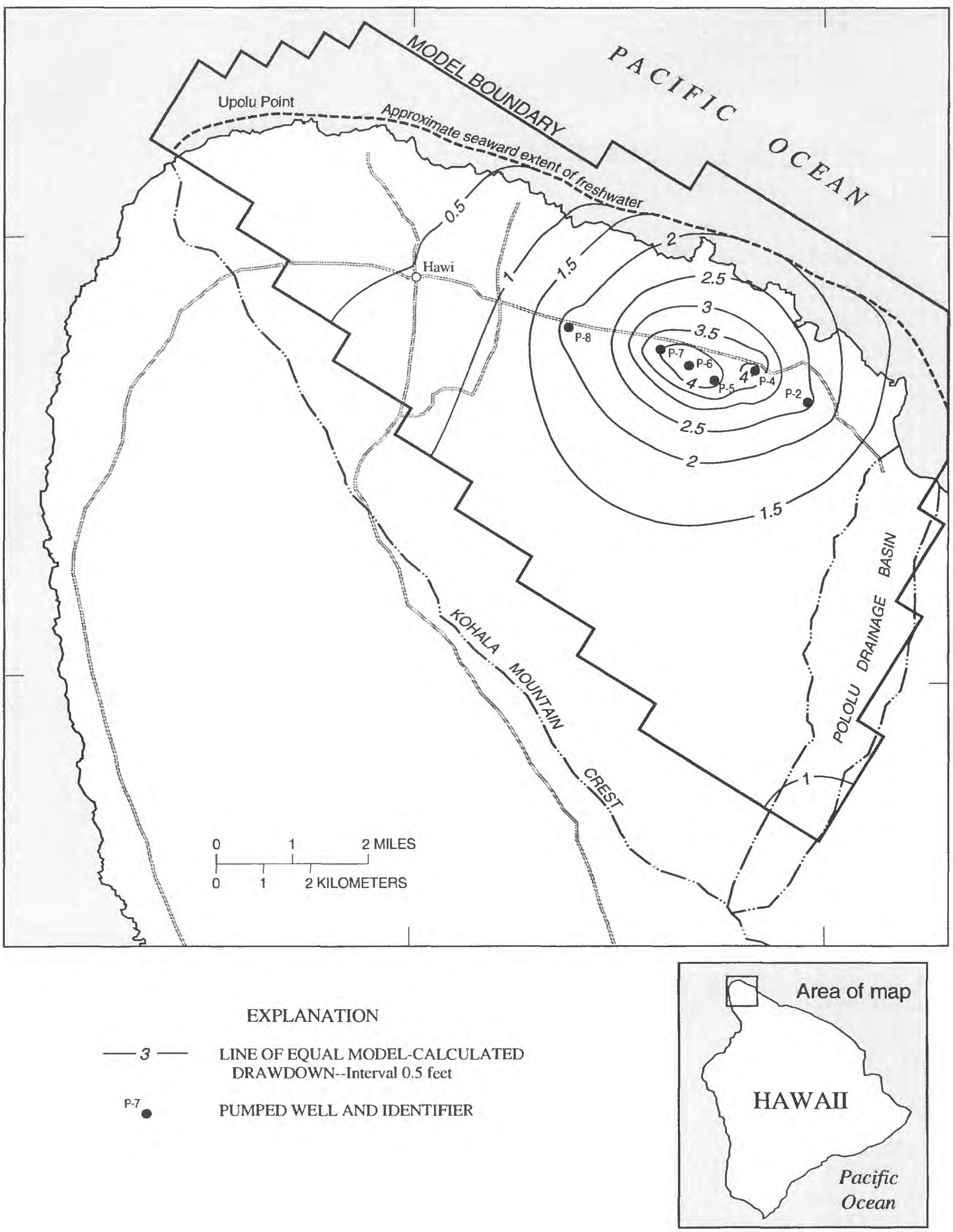

Figure 20. Model-calculated drawdown for pumping scenario 2, Kohala area, island of Hawaii.

Once again, model-calculated decline in water-level in Pololu drainage area is about 1 ft. The termination of the model at the eastern drainage divide of Pololu Stream precludes the induced movement of ground water from the excluded area into the modeled area, which would be presumed to occur under actual pumping conditions. The exclusion of this induced movement of ground water toward the pumping centers results in the model over-estimating water-level declines by about 0.5 ft. Over-estimating water-level declines makes model calculations of ground-water availability conservative.

Model-calculated changes in depth to freshwater-saltwater interface.-- As a result of pumping and subsequent decline of water levels, the freshwater-saltwater interface moves upward. The location of the interface is important because it is the best indicator of the limits on available water at the pumping sites. If the freshwater-saltwater interface rises near or into wells, the salinity of water pumped by the well may increase to levels unacceptable for domestic uses.

The pre-pumping position of the model-calculated freshwater-saltwater interface near the pumping sites is shown in figure 17 and the model-calculated position of the interface resulting from scenario 1 is shown in figure 21. The model-calculated position of the interface resulting from scenario 2 is shown in figure 22. Information on pre-pumping and pumping water levels and model-calculated depth to the freshwater-saltwater interface below sea level are given for each of the simulated pumping nodes in table 6 for scenarios 1 and 2.

The greatest model-calculated decline in water level for scenario 1 is about 3.5 ft at pumping node P-7 and the resulting model-calculated rise in the interface is about 140 ft. Depth to the freshwater-saltwater interface is least (227 ft below sea level) at pumping node P-9. If the thickness of the brackish zone above the interface is assumed to be about 80 ft as indicated at well D, the range in freshwater thickness at the pumping nodes would be about 153 to 252 ft.

The greatest model-calculated decline in water levels for scenario 2 is about 4.7 ft at pumping node P-6 and the resulting model-calculated rise in the interface is about 188 ft. Depth to the freshwater-saltwater interface is least (228 ft below sea level) at pumping node P-7. Using a thickness for the brackish zone equal to 80 ft above the interface as for scenario 1, the resulting range in freshwater thickness from is about 154 to 234 ft.

As discussed previously, wells in basal aquifers are typically constructed to depths ranging from about 50 to 200 feet below sea level. The above results indicate that if ground water is withdrawn in the areas simulated in the two model scenarios, deeper wells (about 200 ft below sea level) would likely experience saltwater intrusion at least at some locations, while shallower wells would tend to maintain a greater buffer of freshwater between the wells and the transition zone. The amount of freshwater buffer would depend on the actual depth, spacing, and pumping rates of these wells. Results also indicate that, as would be expected, the potential for saltwater intrusion increases as pumpage is concentrated.

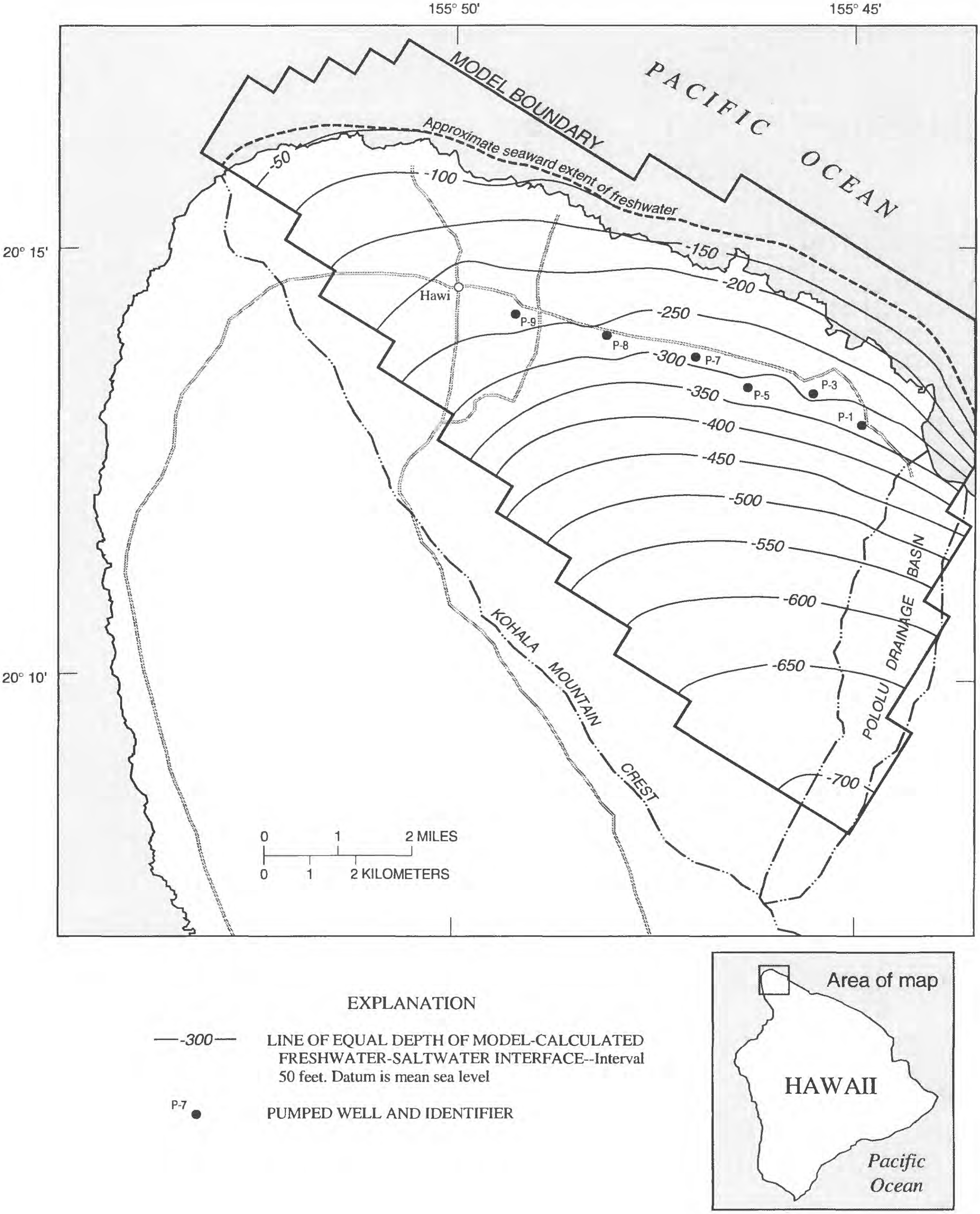

Figure 21. Depth of model-calculated freshwater-saltwater interface for pumping scenario 1, Kohala area, island of Hawaii.

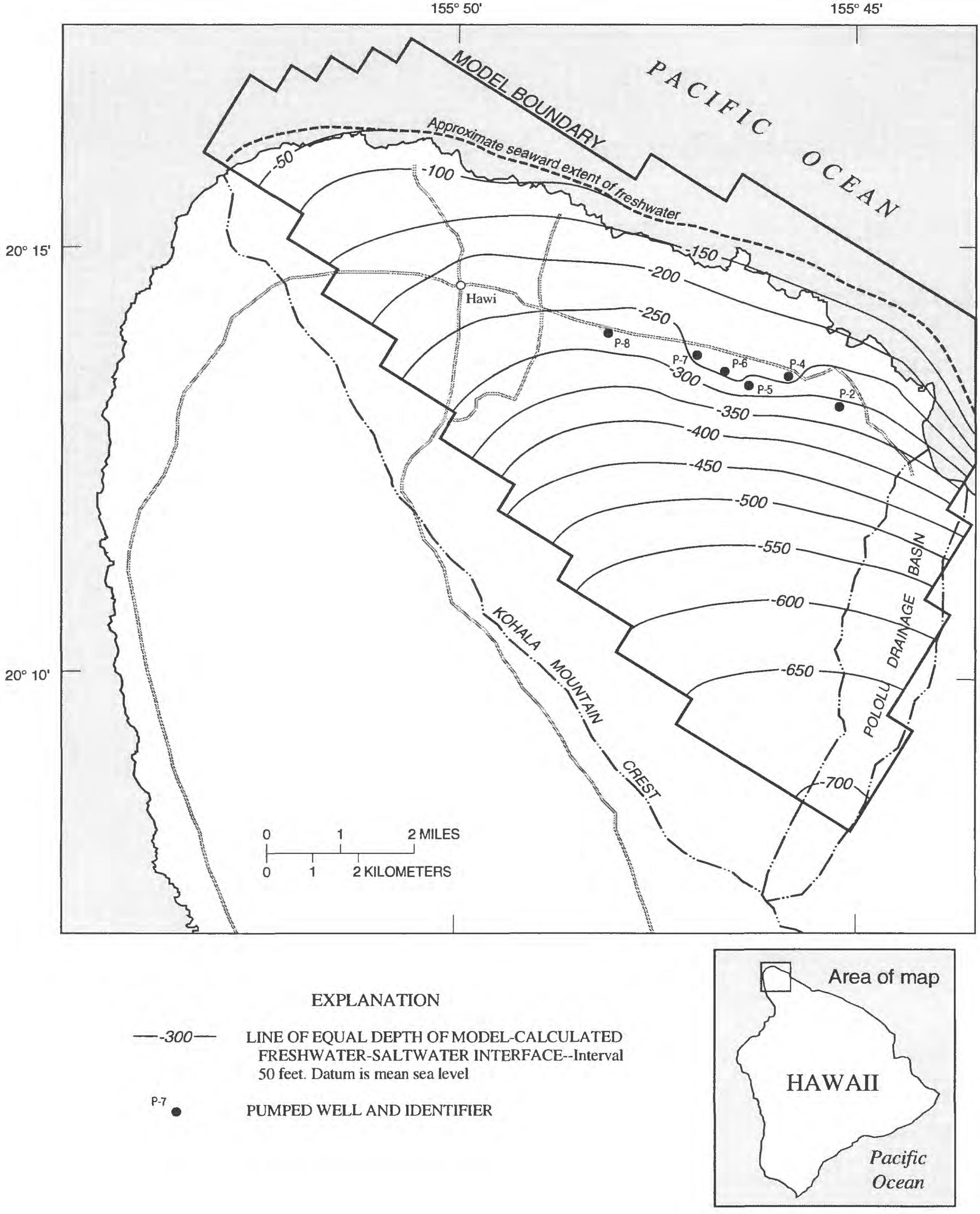

Figure 22. Depth of model-calculated freshwater-saltwater interface for pumping scenario 2, Kohala, Hawaii.

Table 6. Water levels and interface locations at simulated pumping sites, Kohala area, island of Hawaii

Simulated pumping site (fig. 18)	Non-pumping			Pumping			
	Water level (ft above sea level)	Interface depth (ft below sea level)	Approximate thickness of freshwater below water table (feet)	Water level (ft above sea level)	Interface depth (ft below sea level)	Approximate thickness of freshwater below water table (feet)	Water-level change (feet)
				Scenario 1			
P-1	10.3	413	343	8.1	324	252	2.2
P-3	10.3	412	342	7.0	281	208	3.3
P-5	10.9	436	367	7.5	300	228	3.4
P-7	10.1	405	335	6.6	266	193	3.5
P-8	9.0	360	289	5.9	236	162	3.1
P-9	7.0	281	208	5.7	227	153	1.3
				Scenario 2			
P-2	10.3	414	344	7.6	306	234	2.7
P-4	10.1	406	336	5.8	232	158	4.3
P-5	10.9	436	367	6.4	255	181	4.5
P-6	10.5	422	352	5.8	234	160	4.7
P-7	10.1	405	335	5.7	228	154	4.4
P-8	9.0	360	289	6.6	264	191	2.4

Table 7. Steady-state ground-water budget (existing plus simulated pumpage) for the numerical model, Kohala area, island of Hawaii

Sources		Million gallons per day
Direct infiltration of precipitation		60.3
High-level discharge into the basal aquifer		8.1
Kohala ditch seepage		2.0
Hydroelectric plant injection wells		8.0
	Total...........	78.4
Ground-water discharges		
Into ocean		57.8
Existing pumpage		0.6
Proposed pumpage		20.0
	Total...........	78.4

Model results.--The main emphasis of this study was to determine if 20 Mgal/d of ground water can be withdrawn from the Hawi basal aquifer in addition to the existing use of 0.6 Mgal/d. The previous discussion indicates that this withdrawal is feasible, but spacing, depth, and pumping rates of individual wells are an important considerations in planning ground-water development. It is desirable to maintain as thick a body of freshwater beneath the wells as possible.

For existing conditions, water levels range from about 10 ft to 7 ft (see fig. 7) from east to west in the area of simulated pumpage shown in figure 18. Model-calculated steady-state water levels resulting from pumping an additional 20 Mgal/d for scenarios 1 and 2 are shown in figures 23 and 24. As can be seen, water levels are still highest (about 8 ft) in the eastern part of the area of simulated pumpage. Water levels in the western part of the area of simulated pumpage are about 6 ft.

Table 7 shows the components of the steady-state ground-water budget for the modeled area following the simulation of the 20 Mgal/d of additional pumpage for both scenarios. Comparison of table 7 with table 5 indicates that the source of water to the additional pumpage is from reduced ground-water discharge to the ocean by an amount equal to pumpage. Other components of the water budget are the same.

For both pumping scenarios, the model calculates a water-level decline of slightly more than 1 ft near the mouth of Pololu Stream where the stream discharges into the ocean. In this area, it is possible that Pololu Stream is hydraulically connected to the basal aquifer. As a result, a decline in water level near the mouth of Pololu Stream would be sufficient to cause a reduction in streamflow. Because the model terminates along the Pololu watershed boundary, the model would be expected to over-estimate the water-level decline in the area of Pololu Stream, perhaps by as much as 0.5 ft; but even so, the stream would still be affected assuming a hydraulic connection exists with the basal ground-water system.

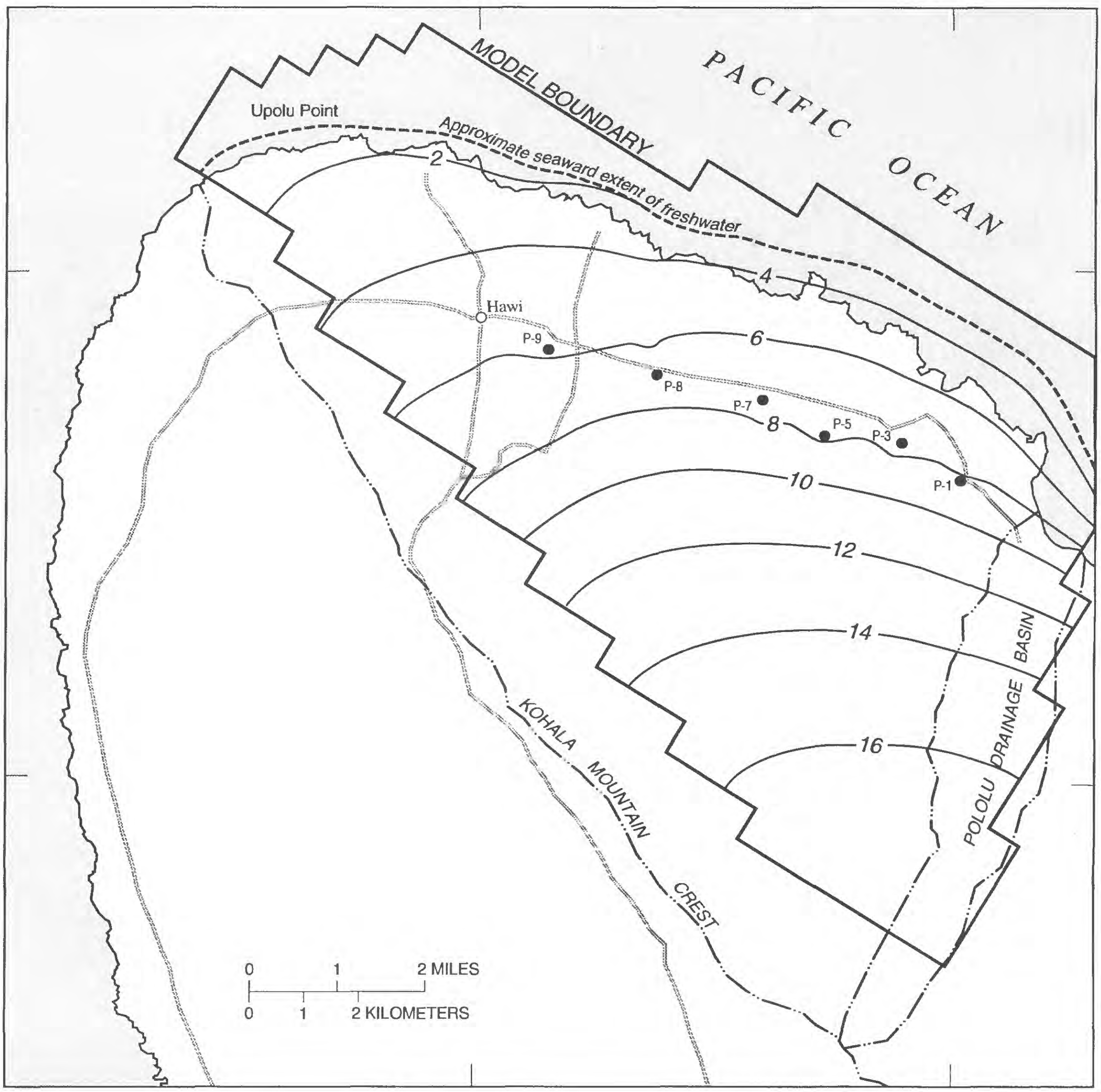

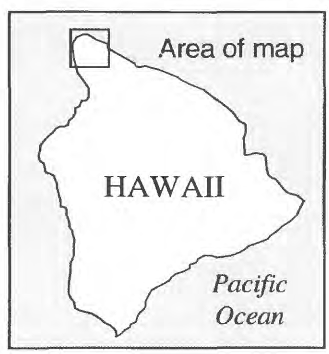

EXPLANATION

— 6 — LINE OF EQUAL MODEL-CALCULATED GROUND-WATER LEVEL--Interval 2 feet. Datum is mean sea level

P-7 ● PUMPED WELL AND IDENTIFIER

Figure 23. Model-calculated ground-water levels for pumping scenario 1, Kohala area, island of Hawaii.

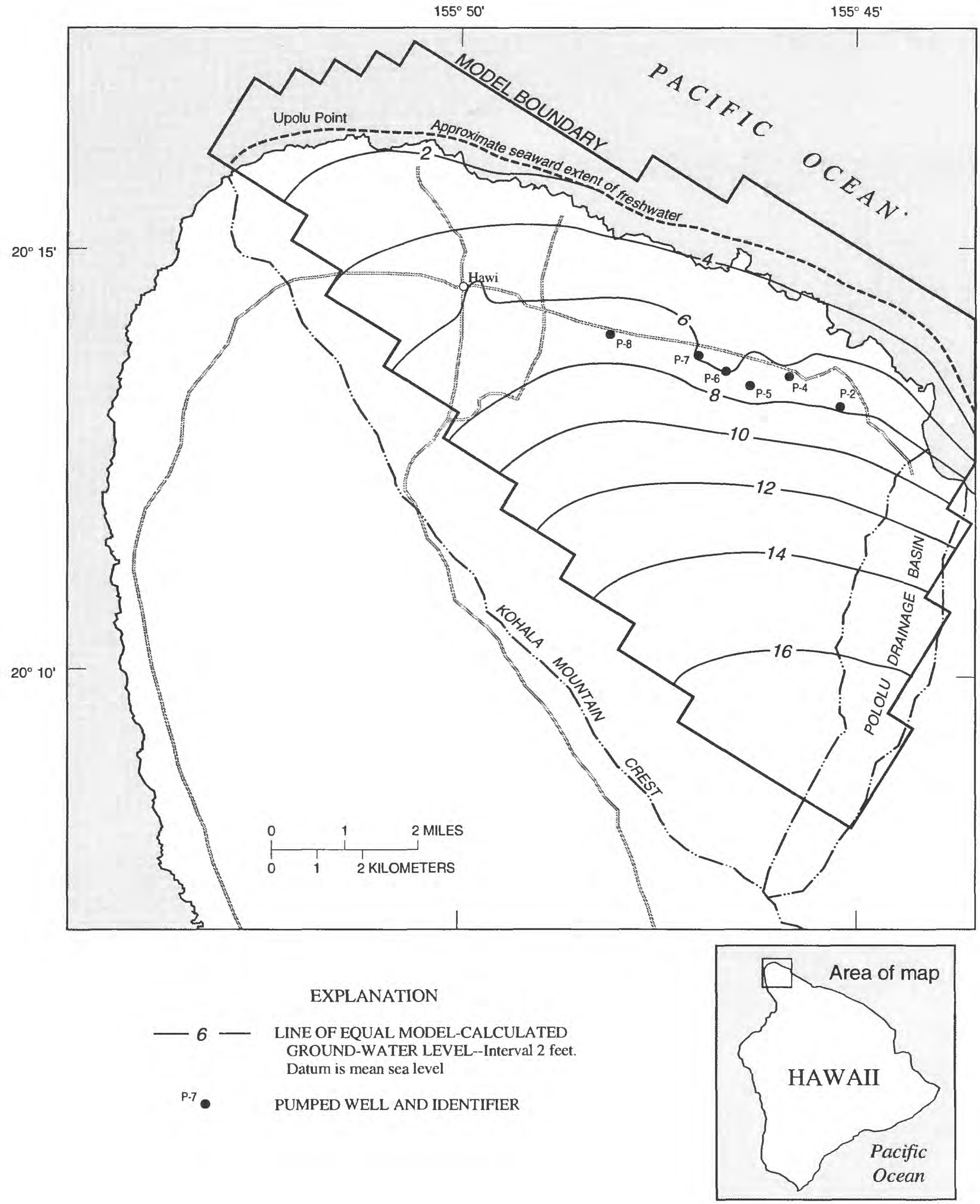

Figure 24. Model-calculated ground-water levels for pumping scenario 2, Kohala area, island of Hawaii.

SUMMARY AND CONCLUSIONS

Model results indicate that ground-water withdrawal of 20 Mgal/d above the existing 0.6 Mgal/d withdrawal at the Hawaii County Department of Water Supply well is feasible from the Hawi basal aquifer, but that spacing, depth, and pumping rates of individual wells are important. If pumping is concentrated, the likelihood of saltwater intrusion is increased. Model results indicate that concentrating as much as 16 Mgal/d in a 1.5 mile stretch roughly parallel to the coast on the eastern side of the basal aquifer, and withdrawing an additional 2 Mgal/d within a mile on either side of this would provide a freshwater thickness of 154 to 234 ft below the areas of withdrawal. In this case, wells with depths of greater than 200 ft below sea level would likely experience saltwater intrusion. If the area of concentrated pumpage is increased from 1.5 to 3 miles and another 2 Mgal/d withdrawn on either side within a distance of about three-quarters of a mile from the area of concentrated pumpage, the freshwater thickness in the area of withdrawal would increase slightly to between 153 and 252 ft.

Under existing conditions, water levels in the basal aquifer range from about 10 to 7 ft above sea level in the area of simulated pumpage. Model results indicate that water levels would range from about 8 to 6 ft above sea level after water-level declines induced by the additional 20 Mgal/d of pumpage stabilized.

The model cannot directly address the subject of individual well yields compared with depth, and this information must be gained from field experience. Even so, it is clear from model results that 20 Mgal/d of additional ground-water withdrawal from the basal part of the Hawi aquifer is possible if pumping centers are spaced adequately apart and well depths are limited.

The withdrawal of 20 Mgal/d would result in a reduction of ground-water discharge to the ocean by an amount equal to pumpage. It is possible that pumping could cause some reduction of streamflow near the mouth of Pololu Stream, but because of a lack of field data concerning the hydraulic connection of this stream with the basal aquifer, the magnitude of the reduction cannot be addressed at this time.

REFERENCES CITED

Akinaka and Associates, Bowles, S.P., and Mink, J.F., 1975, Kohala water resources management and development plan: phase III, Honolulu, Hawaii, 77 p.

Bear, Jacob, 1979, Hydraulics of groundwater: New York, McGraw-Hill, 569 p.

Bennett, G.D., Rehman, A., Sheikh, I.A., and Ali, Sabir, 1967, Analysis of Pumping Tests in the Punjab region of West Pakistan: U.S. Geological Survey Water-Supply Paper 1608-G, 56 p.

Bowles, S.P., Mink, J.F., Akinaka and Associates, and May, C. S., 1974, Kohala water resources management and development plan: phase II, Honolulu, Hawaii, 144 p.

Davis, D. A. and Yamanaga, G., 1963, Preliminary report on the water resources of Kohala Mountain and Mauna Kea, Hawaii, State of Hawaii Circular C14, Honolulu, Hawaii, 44 p.

Eyre, P.R., 1994, Ground-water quality reconnaissance, Tutuila, American Samoa, 1989, U. S. Geological Survey Water-Resources Investigations Report 94-4142, 15 pp.

Fishman, M.J., and Friedman, L.C., eds., 1989, Methods for determination of inorganic substances in water and fluvial sediments: U.S. Geological Survey Techniques of Water-Resources Investigations, book 5, chap. A1, 545 p.

George A.L. Yuen and Associates, Inc., 1992, State water resources protection plan, volumes I and II: prepared for State of Hawaii Department of Land and Natural Resources, 313 p.

Giambelluca, T. W., Nullet, M. A., and Schroeder, T. A., 1986, Rainfall atlas of Hawaii: State of Hawaii, Department of Land and Natural Resources, Division of Water and Land Development, Report R76, 267 p.

Halbig, J.B., Barnard, W.M., Bartlett, S.A., Overfield R.W., and Abbott, L.L, 1986, A baseline study of ground water geochemistry in the Kawaihae and Hilo areas of the Island of Hawaii, State of Hawaii Department of Planning and Economic Development, 74 p.

Harr, M.E., 1962, Groundwater and seepage: New York, McGraw-Hill, 315 p.

Jacob, C.E., 1947, Drawdown test to determine effective radius of artesian wells, American Society of Civil Engineering, Transactions, v. 112, p. 1047-1071.

Langenheim, V.A.M. and Clague, D.A., 1987, Stratigraphic framework of volcanic rocks of the Hawaiian islands, chap. 1 *of* Decker, R.W., Wright, T.L., and Stauffer, P.H., eds., Volcanism in Hawaii: U.S. Geological Survey Professional Paper 1350, v. 1, p. 55-73.

Lau, L.S., 1962, Water development of Kalauao basal springs hydraulic model studies: Board of Water Supply, City and County of Honolulu, 102 p.

Martin, W. F., and Pierce, C.H., 1913, Water resources of Hawaii, 1909-1911: U.S. Geological Survey Water-Supply Paper 318, 552 p.

Moore, J.G.,1987, Subsidence of the Hawaiian Ridge, chap. 2 *of* Decker, R.W., Wright, T.L., and Stauffer, P.H., eds., Volcanism in Hawaii: U.S. Geological Survey Professional Paper 1350, v. 1, p. 85-100.

Polubarinova-Kochina, P. Ya., 1962, Theory of ground water movement: Princeton, N.J., Princeton University Press, 613 p.

Prickett, T.A., 1967, Designing pumped well characteristics into electric-analog models: Ground Water, v. 5, no 4, p. 38-46.

Shade, P.J., in press, Water budget for the Kohala area, island of Hawaii: U.S. Geological Survey Water-Resources Investigations Report 95-4114.

Souza, W.R. and Voss, C.I., 1989, Assessment of potable groundwater in a freshwater lens using variable-density flow and solute transport simulation, in Proceedings of National Water Works Association Conference on Solving Ground Water Problems with Models, Feb. 7-9, 1989, Indianapolis, Indiana.

State of Hawaii, 1970, Basic water resources data: island of Hawaii, Department of Land and Natural Resources, Division of Water and Land Development Report R34, 188 p.

Stearns, H.T. and Macdonald, G.A., 1946, Geology and groundwater resources of the island of Hawaii, Hawaii Division of Hydrography Bulletin 9, 362 p.

Swain, L.A., 1973, Chemical quality of ground water in Hawaii: State of Hawaii Department of Land and Natural Resources, Division of Water and Land Development, Report R48, 54 p.

Thompson, W.Y., 1988, Feasibility study for a Kohala coastal water system, Department of Water Supply, County of Hawaii, 21 p.

Todd, D.K., 1980, Groundwater hydrology (2nd ed.): New York, Wiley, 535 p.

U.S. Environmental Protection Agency, 1991, Drinking water regulations and health advisories: U.S. Environmental Protection Agency, Office of Water, 11 p.

Voss, C.I., 1984, AQUIFEM-SALT: A finite element model for aquifers containing a seawater interface: U.S. Geological Survey Water-Resources Investigations Report 84-4263, 37 p.

Wentworth, C.K., 1939, The specific gravity of sea water and the Ghyben-Herzberg ratio at Honolulu: University of Hawaii Bulletin, v. 18, no. 8, 24 p.

Wershaw, R.L., Fishman, M.J., Grabbe, R.R., and Lowe, L.E., eds., 1987, Methods for determination of organic substances in water and fluvial sediments: U.S. Geological Survey Techniques of Water-Resources Investigations, book 5, chap. A3, 80 p.

GPO 686-022/39174